OVERCOMING CHALLENGES ON HCV GLYCOPROTEINS AND RECEPTORS PRODUCTION: A USEFUL MAMMALIAN CELL EXPRESSION SYSTEM

by

YUANYUAN WANG

A dissertation submitted to the

School of Graduate Studies

Rutgers, The State University of New Jersey

In partial fulfillment of the requirements

For the degree of

Doctor of Philosophy

Graduate Program in Chemistry and Chemical Biology

Written under the direction of

Joseph Marcotrigiano, Ph.D.

And approved by

_____

_____

_____

_____

New Brunswick, New Jersey

January, 2019

ABSTRACT OF THE DISSERTATION

OVERCOMING CHALLENGES ON HCV GLYCOPROTEINS AND RECEPTORS PRODUCTION: A USEFUL MAMMALIAN CELL EXPRESSION SYSTEM

By YUANYUAN WANG

Dissertation Director: Joseph Marcotrigiano, Ph.D.

Hepatitis C is a liver disease caused by hepatitis C virus (HCV). HCV is the major cause of cirrhosis and hepatocellular cancer in the US and is the number one cause of liver transplantation. An estimate of 3.5 million people is chronically infected in the US with 400,000 individuals deaths from chronic HCV infection every year. Several direct-acting antiviral (DAA) agents have been approved by the Food and Drug Administration (FDA). HCV is a blood-borne virus, which prior to 1992 was transmitted through blood transfusion. An estimated 41,200 new cases of HCV infection occurred in the US with an additional 1.75 million worldwide in 2016. Therefore, there is an urgent need to control the transmission of HCV, in addition to the antiviral intervention to limit the spread of the virus. Vaccination is the most effective way to control the infection rate as no infectious disease has ever been eradicated by treatment alone. However, no vaccine is available to prevent HCV infection.

A useful mammalian cell expression system was described to produce HCV envelope glycoproteins E1 and E2, as well as the cell surface receptors, scavenger receptor class B type I (SRB1) and cluster of differentiation 81 (CD81). Our method combines the speed

and high efficiency of lentiviral infection with an adherent cell bioreactor to allow large-scale production of proteins in mammalian cell lines. The full-length ectodomain of HCV E1 was produced at milligram quantity and is recognized by conformational antibodies from patient samples. E1 can associate with the apolipoproteins from the cell culture serum. HCV E2 produced by the mammalian cell expression system has the function to bind cell surface receptors and antibodies. Crystals of E2 and CD81 diffract to 4.3 Å resolution allowing us to produce a low-resolution model of the E2-receptor complex.

Overall, our result extends the current understanding of HCV entry by providing more structural, biophysical, and functional information on the HCV glycoproteins. The studies of the receptor interaction can contribute to vaccine design to halt the spread of HCV infection.

Acknowledgements

Firstly, I would like to express my gratitude to Dr. Joseph Marcotrigiano for being an inspiring and encouraging mentor. He is an energetic scientist who always has great ideas and always open to anything new. Through these four years, he is always patient on teaching me and guiding me not only on science, but also on my career.

Secondly, I would like to thank my committee members Dr. Eddy Arnold, Dr. Jean Baum, Dr. David Case, and Dr. Jeffrey Cohen. Eddy is always providing inspiring ideas on committee meeting which guide me on different approaches to solve the problem. Jean, as a committee member, teaches me to interpret data more thoroughly and critically, and as a director the graduate program, is supportive during my transition time. Jeff encourages me on holding a positive attitude to solve the problem and his door is always open when I need. I appreciate David for his generosity to be on my committee.

Thirdly, my great appreciation is to my excellent lab members. Without the support and help from them, it's impossible for me to finish this thesis. I would like to acknowledge the former members, Dr. Abdul Khan for his patience on training me, Dr. Samantha Yost for the being a supportive neighbor, Dr. Chen Wang for the four-year mental support, and many other past members. I also want to express my sincere appreciation to the current lab members, Myeisha Paskel for being a supportive big sister, Jennifer Casiano-Matos for always stand by me, and many others. It's my real pleasure to work with you all.

Additional thanks to my friends and colleagues at CCB, at CABM, and at LID, Snow Yang, Wen Wu, Yu Liu and many others. I appreciate the constructive suggestions and advice on science and the great help in these four years. I really enjoy the all the interesting

discussion and it's such fun with you all.

I must give recognition to my friends who help me survive my transition period. Thank you all for the support and encouragement, Anxin Bai, Yingfu Lin, Lu Xia, Toan Van Tu, Haiyang Wang, and Livia Fang.

Lastly, many thanks to my parents for their unwavering support, wisdom, and lots of love.

Dedication

This thesis is dedicated to my grandmother. You guided me step by step when I was young and taught me to believe in myself. Every time we meet, you tell me that you're proud of me and how good I am. I'm truly grateful for your love and support.

Table of Contents

List of Figures

List of Tables

Introduction

Hepatitis is defined as inflammation of the liver, which can be caused by viral infection. Hepatitis B virus was discovered in 1967 and hepatitis A virus was discovered in 1973. In 1989, a non-A, non-B hepatitis (NANBH) was characterized in a patient serum. A cDNA library from an NANBH patient was expressed in *E.coli* and probed with various serum samples, providing clinical evidence for NANBH infection. The clones of the cDNA, constructed by patient library, were identified to be derived by RNA molecules during the infection [1]. The cloned genome of a NANBH agent was eventually designated as the hepatitis C virus (HCV), which can be tested by the specific antibodies and PCR based assays in patient blood samples [2]. The discovery of HCV is a breakthrough in virology and the HCV testing methods have further enhanced the safety of the blood supply.

1 Epidemiology

Hepatitis C is a liver disease caused by HCV, which can result in both acute and chronic diseases. Acute HCV infection usually happens in the first six months after exposure for a short-term illness. From 2010 to 2016, the Centers for Disease Control and Prevention (CDC) reported a 3.5-fold increasing in HCV acute infection in US [3]. Approximately 75-85% newly infected patients will become chronic, resulting in a lifelong infection. According to the World Health Organization (WHO), an estimated 71 million people are chronically infected globally [4]. An estimated of 3.5 million people are living with HCV infection within US [5]. It is estimated that around 400,000 individuals die from chronic HCV infection every year.

Symptoms of HCV infection include loss of appetite, abdominal pain, fatigue, nausea,

dark urine, and jaundice. Chronic HCV infection can develop into liver cirrhosis, liver cancer, and death. However, most people are unaware of their infection, since they are asymptomatic. As a result, HCV is the major cause of cirrhosis and hepatocellular cancer in US and is the number one cause of liver transplantation.

Among all the HCV infected patients, 15-25% can spontaneously clear infection without any treatment or medication. The previous treatment consisted of pegylated interferon (PEG-INF) and ribavirin [6]. In 2011, two protease inhibitors, boceprevir and telaprevir, were approved by the Food and Drug Administration (FDA). Since then, several new direct-acting antiviral (DAA) agents have been approved, targeting different HCV nonstructural proteins. Currently, there are 11 FDA approved DAAs available on the market. However, access to DAAs is limited due to the high cost of the treatment.

HCV is a blood-borne virus, which prior to 1992 was transmitted mostly through blood transfusion. Currently, an estimated 41,200 new cases of HCV infection occurred in US with an additional 1.75 million worldwide in 2016 [3]. New infections in US result from injection drug use with an average age between 20-29 [7] [8]. Therefore, there is an urgent need to control the transmission of HCV, in addition to the antiviral intervention to limit the spread of the virus. Vaccination is the most effective way to control the infection rate as no infectious disease has ever been eradicated by treatment alone. However, no vaccine is available to prevent HCV infection.

2 Virology

HCV is a positive-sense, single-strand RNA virus from the genus of *Hepacivirus* in the *Flaviviridae* family. HCV has approximately 9,600 nucleotides of 3,010 amino acids with seven major genotypes (numbered 1-7) [1] [9]. The genome of HCV has the open reading frame (ORF) with the untranslated regions (UTRs) at 5' and 3' ends. The 5' UTR contains 341 nucleotides and an internal ribosome entry site (IRES). The ORF contains around 9,100

nucleotides, encoding into a polyprotein which can be cleaved by different proteases to ten mature proteins, including three for the structure of the virion and seven non-structural proteins for genome replication [10].

The structural proteins of HCV consist of the core, envelope glycoprotein 1 (E1), and envelope glycoprotein 2 (E2). Core is the capsid protein with additional functions in signal transduction and lipid droplet binding [11]. E1 and E2 are on the surface of the virion that mediate the viral entry [12].

The non-structural proteins consist of p7, nonstructural protein (NS) 2, NS3, NS4A, NS4B, NS5A, and NS5B. p7 is an ion channel for virus assembly and release [13]. NS2 plays a role as the auto-protease for NS2 and NS3 cleavage [14]. NS3 is a bifunctional protease/helicase that mediates viral polyprotein cleavage and RNA replication [15], which could be a target for drug design. NS4A is a co-factor of NS3, while the function of NS4B is unclear [16]. NS5A has an interferon sensitive region and is phosphorylated by host kinases [17]. NS5B is an RNA dependent RNA-polymerase [10].

All of the HCV proteins are necessary for viral attachment, entry, fusion, replication, assembly and release. The NS3 protease, NS5A and NS5B are the major targets for approved DAAs.

3 Virion Paricle

Structural information for the HCV particle has been difficult to characterize due to the low levels of viral particle production under laboratory conditions and size heterogeneity of the virions. The cryo-electron microscope (Cyro-EM), negative-stain electron microscope, and electron cryotomography (ECT) demonstrated that HCV virions have a broad, radial distribution between 50-80 nm in diameter with a smooth and even surface [18]. Moreover, HCV virions can interact with host lipoproteins and form into very low-density lipoproteins

(VLDLs) and low-density lipoproteins (LDLs) complexes [19] [20].

4 Viral Glycoproteins

HCV envelope proteins, E1 and E2, play a pivotal role in the HCV replication cycle for receptor binding and virus entry of the host cells. E1 and E2 are located on the outer shell of the virus particle, mediating virus attachment to the target cell and facilitate membrane fusion [12].

E1 and E2 glycoproteins are type I transmembrane proteins that anchor to the endoplasmic reticulum (ER) lumen. The N-terminal ectodomain of E1 and E2 that are highly modified with disulfide bonds and N-linked glycosylations, while the C-terminal transmembrane α-helices are responsible for heterodimer formation and ER retention [21] [22]. The ectodomains of E1 and E2 (eE1 and eE2) are heavily-glycosylated soluble protein, with nearly half of the protein mass contributed by glycans [23]. In addition, eE1 and eE2 contain several intramolecular disulfide bonds [24]. The core structure of the HCV E2 and the N-terminal domain of E1 (nE1) were determined [23] [25] [26], providing the detailed structural information on the HCV glycoproteins.

The crystal structure of N-terminal (amino acid 192-270) domain (nE1) of HCV was determined in 2014, revealing a novel folded dimer [26]. nE1 has a N-terminal β-hairpin followed by a long α-helix and three antiparallel β-sheets containing both inter- and intramolecular disulfide bonds (Figure 1). The nE1 structure does not show structural similarity to any known viral fusion protein.

E2 core from genotype 1a was co-crystallized with a human neutralizing antibody (AR3C) (PDB ID: 4MWF) [25]. While the other crystal structure of E2 was from genotype 2a with a mouse antibody 2A12 which recognizes a linear non-neutralizing epitope on C-terminal (PDB ID: 4WEB) [23]. Alanine scanning studies for mapping the neutralizing

antibody recognition sites was applied on core E2 protein, confirming the reliability of the published structure [27]. Both structures showed a monomer globular conformation with multiple β-sheets stabled by the hydrophobic core and several disulfide bonds. More than half of the E2 structure was formed by flexible loops or even completely unstructured regions (Figure 2).

5 Viral Entry

A complex series of receptors are necessary for HCV attachment, entry, and fusion.

Initial attachment to a host cell involves glycosaminoglycans (GAGs) and low-density lipoprotein receptor (LDLR). GAG is the large polysaccharides expresses on the surface of the most mammalian cells and usually play a role in the attachment for a large number of virus from diverse families [28]. LDLR is expressed in the liver and has a major function of capturing LDL from the blood circulation to import into the liver [29]. Scavenger receptor class B type I (SRB1) can regulate the HCV binding as a downstream factor by interaction with HCV E2 [30]. After the initial viral attachment, lipoprotein rearrangement will undergo to allow the access of the following receptors [31].

In addition, E2 can interact with a critical receptor cluster of differentiation 81 (CD81) to trigger multiple signaling pathway, such as the epidermal growth factor pathway [32]. Claudin 1 (CLDN) and Occludin (OCLN) are members of cellular tight junctions expressed in the liver. Claudin 1 might interact with HCV subsequently to SRB1 and CD81 binding [33]. Occludin was found in the downstream of the CD81 and Claudin 1 binding [34]. These tight junctions play an important role in triggering the membrane fusion (Figure 3).

After endocytosis and internalization, HCV undergoes viral and host membrane fusion to release viral RNA into the cytoplasm. Membrane fusion is dependent on the endosomal acidification [35]. HCV E1E2 was classified into class II fusion proteins which requires a

low-pH induction for membrane merging [36]. The class II fusion proteins, from *alphavirus* and *flavivirus*, can insert vertically into the membrane triggering the pH-dependent conformational change of envelope proteins. Under the endosomal acidification, HCV E1E2 may have a series of rearrangement of both oligomeric and structural changes to form a stable conformation [37] (Figure 3).

Currently, details and evidence of the oligomeric and conformational transition during membrane fusion in HCV entry are poorly understood. Further structural and functional information of E1 and E2 will provide a better mechanistic understanding of HCV entry.

Significance

Understanding the HCV entry mechanism is important for vaccine design to halt the spread of HCV infection. The basic need for patient treatment is to understand the mechanism of how the virus recognizes and enters the target cells, especially the function of HCV glycoproteins during the entry. In addition, structural insights of the interaction between viral surface protein and cell surface receptors would guide the vaccine design strategies.

Overall, this thesis aims to extend the current understanding of HCV entry by applying structural, biophysical, and functional studies on the HCV glycoproteins and receptors.

Method

1 Production of HCV E1 Ectodomain (eE1)

1.1 Plasmid Constructs Cloning

The HCV eE1 protein was cloned into pJG vector, provided by Dr. John Shires from Emory University. The pJG vector consists of a Cytomegalovirus (CMV) promotor, a rev response element, a woodchuck hepatitis promotor response element and a N-terminal prolactin signal sequence to promote secretion and proper trafficking, followed by tandom C-terminal protein A and 3X-Flag tags (Sigma Aldrich) (Figure 4). Four μg of the modified pJG vector was digested by 80 units of BamHI (NEB) restriction enzyme for 16 hours at 37 °C followed by dephosphorylation using Quick Dephosphorylation Kit (NEB) to prevent religation of the linearized plasmid. PCR amplified eE1 gene with the overlapped sequences of the cloning vector, was introduced via InFusion-HD cloning (Clontech) into the linearized pJG vector. The recombinant circular constructs were transformed into the HB101 strain of *E.coli*. All constructs were confirmed by DNA sequencing.

1.2 Lentivirus Production

A 225 cm^2 (T225) monolayer flask with 6.2 million HEK293T cells was seeded in 30 mL Dulbecco's Modified Eagle Medium (DMEM) with 10% Fetal Bovine Serum (FBS). The cells are grown in 37 °C incubator with 5% CO_2 overnight. For transfection, 90 μg pJG-eE1, 60 μg psPAX2 packaging plasmid (Addgene), 30 μg pMD2.G envelope plasmid (Addgene), 450 μL 2 M $CaCl_2$, and q.s. to 4.5 mL of ddH_2O was added together gently and mixed in a 50 mL falcon tube. 4.5 mL 2X HEBS (6.24 g HEPES, 8.18 g NaCl, and 0.11 g disodium phosphate in 500 mL ddH2O) was added by bubbling with a 10 mL serological pipet for 10

seconds, followed by room temperature incubation for two minutes. The reaction mixture was added directly to the media in T225 flask (Figure 5). Media was changed after 6-8 hours with 40 mL DMEM with 10% FBS and 1% Antibiotic-Antimycotic (A/A) (D10 media).

1.3 Lentivirus Infection

Two days later the transfection, 20,000 HEK293S GnTI^{-} (lacking N-acetylglucosaminyltransferase I) cells were seeded in 100 μL DMEM with 10% FBS media into a 96-well tissue culture plate. The next day, the culture supernatant containing lentivirus from the T225 flask was collected into a falcon tube, followed by centrifuge at 4,000 g for 30 minutes at 4 °C. The clarified supernatant was centrifuged at 25,000 rpm for 1.5 hours at 4 °C by Beckman L8-M Ultracentrifuge. The supernatant was discarded and replaced by 120 μL of DMEM with 20% FBS, 1% A/A, and 8 ug/mL polybrene (D20PB media) for re-suspending the virus pellet. A half volume of the virus suspension was added to the 96-well plate to replace the original media. The following day, 150 μL of the fresh D10 media was added to the well. The next day, 200 μL of the D10 media was used to replace the infection well.

1.4 Western Blot

By several passages after the infection, a stable cell line was generated. The supernatant of the cell line was collected and centrifuged at 13,000 rpm for two minutes to remove the dead cells. Two samples were prepared for every supernatant by adding SDS-PAGE loading buffer alone with and without 5% β-mercaptoethanol (BME) as the reducing reagent. The samples were heated at 95 °C for five minutes and loaded onto the 4-20% precast protein gel (Biorad) for SDS-PAGE with the protein marker. The gel was transfer to a nitrocellulose membrane (GE Healthcare) using the semi-dry system. The membrane was blocked by 5% non-fat milk and incubated with 3-5 μg of monoclonal anti-FLAG M2 (Sigma-Aldrich) as the primary antibody overnight at 4 °C, washed with 1X phosphate-buffered saline with 0.05% Tween-20 (PBS-t), and further incubated with goat, anti-mouse horseradish

peroxidase (HRP) conjugate (Southern Biotech) as the secondary antibody for an hour at room temperature. After washing with PBS-t, the membrane was developed with SuperSignal West Pico Chemiluminescent Substrate (Thermo Scientific).

1.5 Bioreactor Seeding

The stable cell line expressing the gene of interest were serially expanded from 96-well plate to three 175 cm^2 (T175) flasks. Once the confluency was reached, the cells were split in D10 media with a total volume of 30 mL. The BelloCell bioreactor (Chemglass) was pre-warmed on the BelloStage (Chemglass) for an hour with 470 mL of D10 media. Thirty mL of the suspended cells were slowly expelled using a serological pipet to distribute evenly over the matrix. The seeded BelloCell was settled on BelloStage for 2-4 hours using a 2 mm/s oscillation rate with a top hold for 20 seconds. Afterwards, the bioreactor was operated with 1 mm/s oscillation rate, top hold for ten seconds and bottom hold for one minute (Figure 6).

1.6 Bioreactor Harvest

Three days after seeding, the media was aspirated from the bottom chamber through the center access of the matrix chamber, using a 2 mL aspiration pipet. A half-liter of the fresh D10 media was added through the same access to the bottom chamber. For regular maintenance, the media was harvest and replaced every other day. The harvested supernatant was centrifuged at 4,500 rpm for 15 minutes at 4 °C and filtered through a 0.2 μm Millex filter (EMD Millipore) to remove the cell debris. One mM sodium azide solution was added to the filtered supernatant, allowing to store at 4 °C for weeks.

1.7 Purification of eE1

Several (2-4) liters of the eE1 supernatant was loaded at a flow rate of 0.5-0.8 mL/min onto an IgG Sepharose column (GE Healthcare) equilibrated with 20 mM sodium phosphate pH 7.0 buffer. After loading, the column was washed with six column volumes of 20 mM

sodium phosphate pH 7.0 buffer and equilibrated with four column volumes of 20 mM HEPES pH7.5, 250 mM NaCl, and 5% glycerol (HEPES buffer).

Rhinovirus (HRV) 3C protease was expressed in *E.coli* cells and purified with a glutathione S-transferase (GST) tag. The purified GST-HRV3C protease was diluted into one column volume of HEPES buffer and slowly injected to the IgG column with a syringe at around 1 mL/min. After two days of digesting, IgG column was connected on the top of pre-equilibrated GSTrap and Q (GE Healthcare) columns with HEPES buffer. eE1 protein was collected in tubes from the column flow-through at the flow rate of 1 mL/min. After collecting eE1 protein, IgG column was cleaned with 0.1 M sodium citrate pH 3.0 and 20 mM KCl.

1.8 Size-exclusion Chromatography (SEC)

A Superose 6 Increase 10/300 GL (GE Healthcare) column was equilibrated with HEPES buffer using AKTA Pure (GE Healthcare) system. Purified eE1 protein was injected to the column with HEPES buffer as the elution buffer.

1.9 Mass Spectrometry

The eE1 samples were gel filtered in 20 mM HEPES pH 7.5 and 150 mM NaCl buffer. Analytical mass spectrometry was performed at the Protein Chemistry Section in Research Technologies Branch (RTB) at National Institute of Allergy and Infectious Diseases (NIAID) using matrix-assisted laser desorption ionization time-of-flight (MALDI-TOF), electrospray ionization time-of-flight (ESI-TOF), and electrospray ionization quadrupole (ESI-Quadrupole) methods. MALDI and intact mass were obtained, and post-data-acquisition analyzed to get the mass of the substance.

1.10 Analytical Ultracentrifugation (AUC)

The eE1 samples were purified and buffer exchanged by SEC, using the elution buffers with different pHs: (a) 20 mM sodium phosphate pH 5.0 with 250 mM NaCl and (b) 20mM sodium phosphate pH 7.0 with 250 mM NaCl.

The experiment was performed at University of Texas Health Science Center at San Antonio (UTHSCSA) for Macromolecular Interactions (CMMI) with Beckman Optima XL-I. Measurements were pelleted at 20 °C for 16 hours at 38,000 rpm and UV absorbance was measured at both 280 nm and 230 nm for concentration determination. Data calculation and analysis was performed at UTHSCSA, using the UltraScan program suite[38].

1.11 Deglycosylation with Endoglycosidase H

Endoglycosidase H (Endo H) was expressed in *E.coli* cells and purified with a GST tag. 1 M sodium citrate pH 5.5 buffer was added to the purified eE1 to a final concentration of 100 mM to lower pH for optimal enzymatic deglycosylation. Based on the ratio, 1 mg Endo H-GST to 2 mg of eE1, Endo H-GST was added to cleave within the chitobiose core of high mannose and some hybrid oligosaccharides from N-linked glycosylation sites. The deglycosylation reaction was incubated at room temperature for 3.5 hours.

1.12 Purification of Deglycosylated eE1

After deglycosylation, the sample was applied to a GST column to separate eE1 from the enzyme. Deglycosylated eE1 collected in the flow-through from GSTrap column followed by Superose 6 Increase 10/300 GL column using HEPES buffer for further purification.

1.13 Negative Stain Electron Microscope

eE1 samples were buffer exchanged to 20 mM HEPES pH 7.5 and 150 mM NaCl buffer by SEC, followed by concentrating to 1-1.5 mg/mL. The 400-mesh copper grids with a continuous carbon film were glow discharged for 40 seconds before use to increase the hydrophilicity. Three μL of the eE1 sample was applied to the grid and removed by blotting with filter paper after incubation for one minute, followed by three times washes with ddH2O. The grid was air dried after adding 3 μL of 2% UranyLess as the stain. The images were required by Gatan 894 TEM operated at 120kV with a UltraScan 1000 CCD camera.

2 Characterize the Structure of eE1 in Complex with Antibodies

2.1 Monoclonal Hybridoma Culture

eE1 monoclonal antibody cell lines (H111 and H114) were provided by Dr. Steven Foung's lab at Stanford Medical School. Hybridoma cells were grown in Iscove's Modified Dulbecco's Medium (IMDM) with 10% low-IgG serum. The following three methods were used to culture eE1 antibodies monoclonals.

a. Spinner Flask

The culture was seeded with $50x10^6$ cells in 100 mL IMDM media with 10% low-IgG serum, 10 mM HEPES pH 7.5 and 1% A/A (low-IgG media) in 500 mL volume spinner flask (Corning) at 100 rpm. The cells were expanded by adding the same volume of existing media every other day. The culture volume was grown to a final amount of 2-4 liters.

b. Shaker Flask

The hybridoma culture was added in low-IgG media at a concentration of 500,000 cells/mL to a shaker flask (Corning) and placed on shaker platform (Corning) at 125 rpm

in 37 °C incubator with 8% CO_2. The culture volume was grown to a liter.

c. Membrane flask

The media layer of CELLine 350 membrane flask (Wheaton) was equilibrated with 10 mL IMDM media with 1% low-IgG serum, and 10 mM Hepes pH 7.5 (nutrient medium). After equilibrating for 10 seconds, $8x10^6$ cells were inoculated to the cell layer of membrane flask in 6 mL IMDM media with 15% low-IgG serum, and 10 mM HEPES pH 7.5. Air bubbles were removed by pipetting up and down for few times. An additional 340 mL of the nutrient medium was added to the media layer of the membrane flask. After 4-6 days of stationary incubation, the hybridoma cells were harvested when the culture grew to $2x10^8$ cells.

The harvested supernatant was centrifuged at 5,000 rpm for 15 minutes and filtered through 0.2 μm PES filter to remove the cell debris. One mM Sodium azide solution was added to the filtered supernatant, allowing to store at 4 °C for weeks.

2.2 Enzyme-linked Immunosorbent Assay (ELISA)

Nunc-Immuno MicroWell 96-Well plate (Thermo Scientific) was coated with 10, 5, and 2.5 μg eE1 solution diluted in 50 μL of PBS-t in each well and incubated at 4 °C overnight on a circular rocker. Each well was replaced by 100 μL of 5% BSA as a blocking buffer followed by three washes with PBS-t. After an hour of blocking at room temperature, 50 μL of the antibody culture supernatant was added as the primary antibody and incubated for another hour at room temperature. Anti-mouse HRP was introduced as the secondary antibody at 1: 15,000 dilution in PBS-t for one hour at room temperature. Finally, the plate was developed by 50 μL TMB (3,3',5,5'-Tetramethylbenzidine) substrate (Thermo Scientific) for five minutes followed the addition of 50 μL of 2 M sulfuric acid to terminate the reaction. The absorbance at 450 nm was quantified by Softmax Pro software on SpectraMax i3x (Molecular Devices).

2.3 Purification of Monoclonal Antibodies

The filtered hybridoma culture media was loaded onto a Protein G column (GE Healthcare) which was pre-equilibrated with 4-6 column volumes of 20 mM sodium phosphate pH 7.0 buffer. After loading, the column was washed with another 4-6 column volumes of 20 mM sodium phosphate pH 7.0, followed by four column volumes of 1XPBS. The antibody was eluted with 0.05% trifluoroacetic acid (TFA) directly into 1 M Tris-HCl pH 9.0 buffer at a volume ratio of 5:1 for immediate neutralization. The purified antibody was dialyzed into 20 mM sodium phosphate pH 7.0 and 10 mM EDTA.

2.4 Antibody Digestion and Antigen-binding Fragment (Fab) Purification

L-cysteine was directly added to post-dialyzed antibody solution to a final concentration of 20 mM. Insoluble papain agarose (Sigma) was suspended in 50 mM sodium acetate pH 4.4 containing 0.01% sodium azide, added at 0.15 mg per 1mg of antibody, and incubated on the tube revolver (Thermo Fisher) for 3-5 hours at 37 °C. The reaction tube was centrifuged at 3,500 rpm for ten minutes followed by filtered by 0.2 μm Millex filter unit to remove the enzyme. Digested Fab was purified using rProtein A Sepharose column (GE Healthcare), eluted with 0.05% TFA, and desalted into 20 mM Tris-HCl pH 8.0. Fab was loaded to Mono Q 5/50 GL column (GE Healthcare) in 20 mM Tris-HCl pH 8.0 and eluted using a salt gradient from 0 to 2 M NaCl.

2.5 eE1/Antibody Complex

eE1 was incubated with antibody Fab at 1:1.2 molar ratio for an hour on ice. The complex was loaded onto a Superose 6 Increase 10/300 GL column using 20 mM HEPES pH 7.5 and 100 mM NaCl as the elution buffer. The complex was concentrated to 7-12 mg/mL by Amicon Ultra-4 Centrifugal Filter Unit (Millipore).

2.6 Crystallization Screening

The initial crystals were grown in commercial screenings from Hampton Research and Molecular Dimensions by the sitting drop vapor diffusion method [39]. After adding 60 μL solution to the reservoir of Intelli-Plate 96, 200 nL protein was added to the sub-well with an equal volume of reservoir solution. Crystallization trials were incubated at both 4 °C and 20 °C for up to several months.

Optimization of Crystals The crystals were grown by the hanging drop vapor diffusion method in 24-well VDX plate with a serial of gradient concentration solutions [39]. After adding 500 μL solution to the reservoir, 1 μL of protein was added onto the 22 mm cover slide (Hampton Research) with an equal volume of reservoir solution. Crystal drops were sealed and incubated at both 4 °C and 20 °C up to months.

3 Characterization of E2 Ectodomain (eE2)

3.1 eE2 Construct Cloning, Expression, and Purification

pJG-eE2 was cloned, expressed, and purified as described in Materials and Method Section 1.

3.2 Purification of Deglycosylated eE2

After deglycosylation reaction, eE2 was desalted into 20 mM Hepes pH 7.5, 50 mM NaCl, and 5% glycerol. Deglycosylated eE2 and the enzyme was loaded onto Heparin column (GE Healthcare). Endo H-GST was separated in the flow-through of the column, while deglycosylated eE2 was eluted using a salt gradient from 0 to 2 M NaCl.

4 Characterization of Cell Surface Receptor CD81

4.1 CD81-LEL Construct Cloning, Expression, and Purification

pJG-CD81-LEL was cloned, expressed, and purified as described in Materials and Method Section 1.

4.2 Isothermal Titration Calorimetry (ITC)

Isothermal titration calorimetry (ITC) experiments were performed by MicroCal iTC200 at Biophysics Core of the National Heart, Lung, and Blood Institute (NHLBI). HCV eE2 was loaded into the cell at around 15 μM, and CD81 was in the syringe at around 100 μM. CD81 was injected into the cell for 17 times (0.2 μL for the first injection followed by 16 injections of 2.35 μL) with stirring at 750 rpm. Titration curves were analyzed with MicroCal AddOn of Origin 7.0 software (OriginLab).

4.3 SEC of eE2 and CD81-LEL Complex

The following complexes were incubated on ice for an hour, (a) eE2 with CD81 at 1:1, 1:2, and 2:1 molar ratio and (b) eE2/Fab with CD81 at 1:1, 1:2, and 2:1 molar ratio. The complex was loaded onto a Superdex 200 Increase 10/300 GL column using elution buffers at different pHs, a) 20 mM HEPES pH 7.5 and 100 mM NaCl, b) 20 mM sodium acetate pH 5.0 and 100 mM NaCl.

5 Crystallization of eE2 in Complex with Antibodies and Cell Surface Receptors

5.1 Complex of eE2, Antibody Fab, and CD81-LEL (E1/Fab/CD81)

Fully-glycosylated eE2 was incubated with antibody Fab at 1:1.2 molar ratio for 1 hour on ice. The E2/Fab complex was loaded onto a Superdex 200 Increase 10/300 GL

column using 20 mM HEPES pH 7.5 and 100 mM NaCl as the elution buffer, followed by concentration to 7-12 mg/mL by Amicon Ultra-4 Centrifugal Filter Unit. CD81 was gel filtered separately and concentrated to 16-20 mg/mL. E2/Fab complex and CD81 was incubated at 1:1.2 molar ratio for another hour on ice to form the complex for crystallization.

5.2 Crystallization Screening

The initial crystals were grown in commercial screenings from Hampton Research and Molecular Dimensions by the sitting drop vapor diffusion method [39]. After adding 60 μL solution to the reservoir of Intelli-Plate 96, 100 nL of the complex, E2/Fab/CD81, E2/Fab, and CD81 were added into the 3 sub-wells individually as well 100 nL of reservoir solution. E2/Fab and CD81 samples were used as negative control. Crystals were incubated at both 4 °C and 20 °C for several months.

5.3 Optimization of Crystals

The crystals were grown by the hanging drop vapor diffusion method in 24-well VDX plate with 500 μL of well solution with a gradient concentration [39]. One μL of the complex was mixed with an equal volume of reservoir solution, consisting of 0.2 M sodium acetate trihydrate pH 4.6 with 14% polyethylene glycol (PEG) 3,350. Single, football-like crystals were formed overnight at 4 °C and kept growing for another three days.

5.4 SDS-PAGE of Crystals

Around ten crystals were transferred to a new drop of mother liquor solution to remove the traces of the protein solution. The transfer step was then repeated for four times to wash the crystal surfaces. The washed crystals were dissolved in SDS-PAGE loading buffer, followed by analysis by SDS-PAGE.

5.5 Cryo Test and Data Collection

Crystals were cryoprotected using reservoir solution supplemented with 25% (v/v)-2-Methyl-2, 4-pentanediol and flash cooled in liquid nitrogen.

Diffraction data was collected at beamline ID-22 from Argonne National Laboratory.

5.6 Structure Determination and Refinement

The data was integrated and scaled by MOSFLM. Phases were determined by the molecular replacement method on PHENIX using E2 core/Fab (PDB ID: 4WEB) and CD81-LEL (PDB ID: 1G8Q) structures. The model was improved by rounds of density modification using COOT and PHENIX. The finally graphics were generated using the program PyMOL.

5.7 Additive Screening

Additive screening (Hampton Research) was set up with 24-well VDX plate using the same crystallization reagent [40]. One μL of the sample was added onto the cover slide followed by 0.8 μL of the crystallization reagent and 0.2 μL of the additive. For the volatile reagent, the additive was added at 10% of the well volume directly to the well solution followed by sealing the reservoir.

6 Characterization of Cell Surface Receptor SRB1

6.1 SRB1 Construct Cloning, Expression, and Purification

pJG-SRB1 was cloned, expressed, and purified as described in Materials and Method Section 1.

6.2 SRB1/Antibody Binding

Anti-SRB1 antibodies were provided by Dr. Maria Teresa Catanese at Nouscom.

Results

1 Characterization of the HCV E1 Ectodomain

After decades of the study, the functions of HCV E1 during viral entry remain unclear [41]. Overall, E1 is known to play an important role in membrane fusion together with E2 [42]. E1 has a role in receptor binding and heterodimer formation with HCV E2. Binding of CD81 to E1E2 complex is stronger when compared to E2 alone, revealing that E1 may mediated the interaction to the cell surface receptor [43]. Furthermore, a conformational human monoclonal antibody (CBH-2) can recognize E1E2, suggesting that E2 may have a different confirmation or undergo structural change with the presence of E1 [44]. Several antibodies have been found against E1 that can neutralize virus entry [45], such as human antibody H111 [46], IGH526 [47], and mouse antibody A4 [48].

Different groups of researchers have been able to express E2 alone and E1E2 in different cell lines. However, attempts to express E1 alone in both mammalian and *Drosophila* systems have yielded mostly misfolded aggregates [49]. E1 is dependent on the downstream sequence of E2 for proper folding and assembly [50] [51]. It has been hypothesized that E2 has chaperone role on co-expression with E1 to help form a native and functional conformation.

Using a novel expression system developed in our lab, our lab has successfully expressed and purified milligrams of properly folded eE1 in mammalian cells in the absence of E2.

1.1 Lentivirus Plasmid Design

Following our success with the production HCV eE2, we explored the use of a similar mammalian cell expression system combined with lentivirus transfection method to produce eE1 glycoproteins.

eE1 fragment was followed by a HRV3C protease site to allow the cleavage of the target protein from a C-terminal affinity tags, protein A and 3XFLAG. The final expression sequence of the eE1 protein includes the prolactin signal, Gly-Ser from the BamHI restriction site, eE1 protein and few amino acids left of 3C protease site. Protein A tag can facilitate protein folding, solubility and purification. HRV3C protease can recognize a specific amino acid sequence as Leu-Glu-Val-Leu-Phe-Gln//Gly-Pro and cleaves between Glu and Gly. Once the protease is loaded to the IgG sepharose column, the protein A tag would remain attached, while untagged soluble eE1 is eluted from the column.

1.2 Production of Stable Cell Lines

Transient DNA transfection is a common method for recombinant protein expression in mammalian cells [52]. The transient transfection allows expression for a limited period of time, it can be lost by cell division and other environmental factors since the DNA is not integrated into the host genome. For long-term large scale protein production, this procedure needs to be repeated for several rounds to get the desired amount of protein. The repetitive nature means that transient transfection is costly and time intensive.

Lentivirus transfection is a safe and quick mean to establish a stable expression cell line [53]. Lentivirus is from *Retroviridae* family, which is able to infect mammalian cells by introducing reverse-transcribed viral RNA into host DNA using viral-encoded integrase enzyme. A transfer plasmid, a packaging plasmid, and an envelope plasmid were introduced by calcium phosphate method to produce pseudotype lentivirus for only a single round of infection. The transfer plasmid, pJG, consists of the target protein followed by an IRES

expressing green flurorescent protein as a visible marker. The packaging plasmid, psPAX2, has encodes HIV Gag/Pol replication and packaging proteins. The envelope plasmid, pMD2.G, encodes vesicular stomatitis virus glycoprotein (VSV-G) to enhance cell tropism and stability.

The multiplicity of infection (MOI) of this method is about 1,000-10,000 to introduce a high number of expression cassettes into the cells. To summarize, the lentivirus system is more efficient means to produce a stable cell lines as it does not (a) require special media or drug selection and (b) need to perform clonal cell lines isolation [53].

1.3 Bellocell Bioreactor

Compared to roller bottle, Cellstack (Corning), and shaker flask, BelloCell bioreactor uses less disposable material saving money and incubator space. BelloCell consists of a bello with a center cage filled with BioNOC II three-dimensional matrices for adherent cell growth. BelloStage holds four bioreactors and has a programmable cable that controls the rate of rising and descending of the bellos. When the stage descends to the bottom, the cells are exposed to the air for aeration. When the stage rises to the top, the cells are in direct contact with the media to uptake nutrients. The cells in the BelloCell can be maintained for up to 3-4 months with continuous media harvest and replacement. Growing cells in BelloCell bioreactor yields “a 10-fold increase compared to the more traditional roller bottle method”.

1.4 Constructs Optimization and Expression Testing

E1 has an ectodomain of approximately 160 amino acids followed a transmembrane domain [54] (Figure 7). The transmembrane of E1 functions as a signal for ER localization and involves in ER retention. The hydropathy characterization suggested that the transmembrane domain of E1 started at amino acid 353 [55]. (Note: amino acid residues of E1 and E2 will be given relative to the first amino acid in the HCV polyprotein.)

In 2014, the crystal structure of N-terminal domain of eE1 (the first 79 amino acids, nE1) was determined (Figure 1). Amino acid 303 on E1 is predicted to be the end of a parallel β-coupling strand [56]. E1 192-311 was successfully expressed and secreted in both mammalian cells and insect cells, but in a misfolded form [57]. Sindbis virus-HCV recombinant E1 192-330 was expressed in Baby hamster kidney-21 (BHK-21) cells with secretion and properly folding [58]. A NMR structure of the transmembrane proximal region eE1 (amino acid 314-342) has been reported (PDB ID: 2KNU) in an α-helical structure with an essential role in membrane fusion [59]. To test the expression of different truncated eE1, nE1, cE1 (amino acid 271-352), E1 192-303, E1 192-311, E1 192-330, and E1 192-342 were expressed in our mammalian system for comparison and further characterization (Figure 7) (Table 1).

Amino acid 262-290 of eE1 was predicted to be a second membrane anchor as well as the membrane fusion peptide during the HCV entry. This region has been hypothesized to be flexible and exposed on the protein surface, driving the conformational change for membrane fusion [60]. It was hypothesized that this hydrophobic region may cause problems in protein expression. To increase the stability of the construct and the bioactivity of the protein, amino acid 263-287 was deleted and replaced by a Gly-Ser-Gly-Ser linker. The most common flexible linker sequences consist of Gly and Ser residues, due to the small and soluble nature of amino acids. By linking the functional domains together, the expression levels and the folding may be improved. Based on the reasons above, eE1 192-352 (full-length ectodomain) linker, 192-311 linker, 192-330 linker, and 192-342 linker constructs have been cloned and expressed (Figure 7) (Table 1).

The expression level and SEC of various E1 fragments and deletions showed that shorten the construct from C-terminal results in lower production. Though 192-352 linker has a better SEC profile with better expression level (Figure 8), the long deletion of the amino acids in the middle of the construct may cause the conformational difference to the native eE1.

Regardless of the previous failure expression trial of full-length eE1 by other groups, it is worth to test the full-length eE1 construct using our system. eE1 192-352 precedes on SEC and Western Blot of expression level than 192-352 linker protein, however, tends to aggregate and precipitates over time.

The His at amino acid 352 of eE1 is known to be important for structure and heterodimer conformation and is highly conserved among different genotypes (Figure 9) [61]. The Trp at amino acid 353 is also conserved and known as a common amino acid in α-helix as well as His. It's highly possible that both His and Trp are parts of the α-helix structure. The construct of eE1 was extended to amino acid 357 to include the conserved His and Trp to help folding to complete the α-helix structure. Surprisingly, by adding five more amino acids on the C-terminal eE1, the homogeneity and production of the protein was improved (Figure 10B). Compared to eE1 192-352, eE1 192-357 is more stable when left at 4 °C for extended periods of time.

In conclusion, eE1 192-357 would be a good candidate to use for the following characterization and crystallization trial.

1.5 Association of eE1 and Apolipoproteins

HCV virion is known to associate with lipoprotein components [62]. Apolipoproteins regulate lipid transportation and metabolism, which plays an important role during the HCV life cycle. Apolipoprotein A-I (ApoA-I) is the major protein component of high-density lipoproteins (HDL), also known as an SRB1 binding ligand, and can mediate viral the RNA replication [63]. Apolipoprotein A-II (ApoA-II) is a major protein component of HDL and is recognized as a hepatic lipase regulator [64]. The purified enveloped HCV virion particles have been visualized by negative-stain electron microscope [65] [18], which turns out that apolipoproteins (ApoA I, ApoB, and ApoE) can associate with serum-derived HCV particles. Moreover, by comparing the immunolabeling accessibility of the host apolipoproteins and HCV glycoproteins, the apolipoproteins are exposed on the surface

and may mask the viral particles.

The purified Con1 eE1 192-352 protein was applied on the SDS-PAGE with reducing and non-reducing conditions, followed by Coomassie staining (Figure 10A). The two major bands were isolated for protein identification at Biological Mass Spectrometry Facility of Robert Wood Johnson Medical School at Rutgers, the State University of New Jersey. The lower band (around 27 kDa) was identified as bovine ApoA-I, which is found in the FBS used in culturing the cells, whereas eE1 localizes on the top band.

The purified eE1 from other HCV genotypes 1b, 3a, and 5a were determined by intact mass spectrometry from the core facility at NIH. Residues of ApoA-I and ApoA-II were identified in all three different genotypes by reverse phase HPLC. The most identified residues are the truncated ApoA-I at amino acids 25-265 and the truncated ApoA-II at amino acids 24-99 (Table 2). In conclusion, E1 was associated ApoA-I and ApoA-II from the culture media. Furthermore, the SEC profile showed a symmetric sharp peak, suggesting eE1/apolipoproteins is a stable complex (Figure 10B).

1.6 pH-triggered Conformational Changes in eE1

Many viral envelope glycoproteins undergo the a low-pH induced conformational change that triggers membrane fusion. The crystal structure of pre- and post-fusion flavivirus envelope (flavivirus E) proteins was determined, suggesting a transition from anti-parallel dimer to vertical trimer against the lipid bilayer. The fusion peptide is exposed at one end of trimer at low-pH, which is a common feature for class II fusion protein [66].

HCV glycoproteins have been reported to undergo a similar conformational change with the low-pH treatment [36]. One evidence of the pH-triggered change of HCV glycoproteins is the different abilities on antibodies and receptors recognition [67]. During endosomal acidification process of HCV entry, the pH range would be 4.5-6.5. Previous work in our lab has shown that E2 does not undergo major oligomeric or structural rearrangement at

low pH by SEC and small angle X-ray scattering (SAXS) analyses, which excludes E2 alone would be the membrane fusion protein in the process [23]. This brought us the hypothesis whether E1 alone could play the direct role in membrane fusion process.

To begin with, the eE1 complex was incubated with pH 5.0 and pH 7.0 buffer followed by SEC to determine the size and oligomeric state of proteins (Figure 11). Proteins with different pHs were at similar elution volumes, suggesting that pH changes do not cause the major oligomeric changes. However, the oligomeric state of eE1 could not accurately be determined by SEC, given that the glycans of eE1 may interact with SEC column resin.

As an alternative approach, AUC was used to determine the oligomeric states of eE1 at different pHs. AUC is a highly accurate technique for determining the molecular weight of a natively folded protein in without any standards or matrix interactions [68]. The size and shape of the protein in solution, as well as some thermodynamic parameters can be measured by AUC, including the molecular weight, equilibrium constant and the species present in solution and their interactions. The result has shown the continuous distribution in molecular weight of the eE1/apolipoproteins complex in both pH 5.0 and pH 7.0 (Figure 12). The sedimentation coefficient distribution of macromolecules can be converted to molar masses distribution, which resulted in better resolution and sensitivity. Other methods of data analysis also agreed in this curve, such as by Van Holde-Weischet plots.

Overall, the molar mass suggests the presence of a more than four components mixture for this stable complex. Interestingly, eE1/apolipoproteins complex undergoes a subtle conformational change at low pH, showing a 3 kDa mass difference. Based on our calculation, E1 and ApoA-I might form a dimer complex along with ApoA-II. At pH 5.0, a small amount of protein might be able to form a trimer complex, shown a small peak around 150 kDa. In the concentration range which has been measured, there is no detectable mass action occurring. If there is an equilibrium of the complex binding, the concentration of the protein sample should be quite far from the dissociation constant (K_d)

of the eE1/apolipoproteins complex. In other word, the binding of eE1 and apolipoproteins is quite strong, so the actual K_d value is much lower than the protein concentration at the equilibrium.

1.7 Negative Stain Electron Microscope of eE1/Apolipoproteins Complex

Negative stain electron microscope is a powerful tool in structural biology. By applying a layer of dried heavy metal solution on the specimen, the contrast and the signal-to-noise ratio would increase for visualization of the specimen. Different views of negative-stain images can be combined for 3D reconstruction. This method undergoes a quick and easy process on specimen preparation to acquire the detailed conformational information. Moreover, by enhancing the contrast, relatively small particles can be visualized under the transmission electron microscope.

For sample preparation, 400-mesh copper grids were coated with a thin layer of continuous carbon film, followed by glow discharging. The support films must be transparent and mechanically stable during the exposure to obtain the good conductivity and help spread of the adherent sample [69]. The particle number can be affected by the incubation time while adding sample to the grids. Washing of the grids will help to remove the salt and macromolecules, especially those components that can interact with stain solution. The heavy metal stain not only enhances image contrast, but also protects the sample from collapsing. To reveal different features of the particles, multiple stains were used. For the negative stain of eE1/apolipoproteins complex, UranyLess and uranyl acetate were both applied. UranyLess is a neutral solution with pH value around 6.8, whereas Uranyl Acetate is acid solution with a pH of 4.2-4.5. To determine whether eE1/apolipoproteins complex would undergo the conformational change, different pHs of the stain solution were tested.

The images were acquired at 120 kV with Charge Coupled Device (CCD) detector. eE1/apolipoproteins complex particles size is around 10-14 nm in a global shape (Figure

13). Human ApoA-I forms a dimer complex in the presence of HDL in a belt ring-like lipid-bound form of structure [70]. It's plausible that ApoA-I forms the ring-like structure, while eE1 takes up the space in the middle of the ring (Figure 14). This model matches our mass spectrometry result, that apolipoproteins would be on the surface of eE1 acting like a protective shell.

1.8 Deglycosylation Test of eE1/Apolipoproteins Complex

N-linked glycosylation occurs in a variety of eukaryotic organisms and is the most common protein post-translation modifications (PTMs). All N-linked glycans are based on the common core pentasaccharide, $Man_3GlcNAc_2$, occurring during the protein synthesis [71]. The consensus sequence of the N-linked glycosylation is Asn-X-Thr and Asn-X-Ser, where X represents any amino acid except Pro.

eE1 has five predicted N-linked glycosylation sites among different genotypes [72]. Different glycosidases are available for deglycosylation of eE1. Peptide-N-glycosidase F (PNGaseF) can remove all types of N-linked glycosylation indiscriminately. The endo-glycosidases such as Endo F1, endo F3, and Endo H, can cleave high mannose and some hybrid glycans and leave only one N-acetylglucosamine (GlcNAc) linked to Asn (Figure 15). Usually, glycans removal results in the less protein flexibility, and the higher degree of homogeneity, which can assist in protein crystal formation and diffraction resolutions. Deglycosylation may avoid the heterogeneity of the glycans of eE1 to help the structure determination.

The deglycosylation reaction conditions vary from different proteins, but the main standard is to enhance the accessibility of the glycosidases enzymes to the glycoproteins. In our case, eE1 protein was diluted around 1 mg/mL and Endo H was added at a 2:1 mass ratio (E1: Endo H). The pH value of the reaction buffer was reduced to pH 5.0 for optimal enzyme efficiency. Heating the reaction up to 37 °C may decrease the solubility of deglycosylated eE1, so the reaction was incubated at room temperature. A sample is

taken at every half an hour and visualized by SDS-PAGE gel to monitor the deglycosylation reaction. A Coomassie-stained SDS-PAGE of the eE1 complex before and after the reaction showed that glycans on eE1 could be cleave by Endo H in four hours (Figure 16).

For the post-deglycosylation purification, the ion-exchange column was usually used as exposure of surface charge after the N-linked glycans are removed. In our case, the main goal is to separate the deglycosyted protein from the enzyme, since there is not much glycosylated eE1 after the reaction. After trying several columns, GSTrap column (to remove the GST tagged Endo H) followed by SEC was selected for further purification (Figure 17).

Homogeneity and solubility are the two major problems associated with the deglycosylated proteins. From the SDS-PAGE and SEC profile, deglycosylated eE1 is shown as a clear band on the gel and a single sharp peak on the chromatography, suggesting deglycosylated eE1 is a relatively homogenous protein (Figure 17). Even with the charge changes on protein surface with glycans removal, deglycosylated eE1 was soluble at both low pH and neutral pH buffers.

For the deglycosylation trial, different conditions and purification methods were applied for different eE1 samples, revealing a protein surface charge and biophysical differences among different constructs. Deglycosylated eE1 from three different genotypes (1b, 3a, and 5a) were analyzed by mass spectrometry to determine the number and distribution of glycans. The deglycosylated eE1 was heterogenous due to the different utility of glycosylation sites. Interestingly, the last glycosylation site (Asn142) was not utilized by all three genotypes.

1.9 Discussion

Full-length, folded soluble eE1 was successfully produced using our mammalian cells expression system without the presence of E2, yielding a solid foundation for continued

biophysical and structural studies.

Considerable time was spent trying to produce eE1 without apoplipoproteins. None of the methods were successful, suggesting a very strong binding affinity between these proteins. Using serum-free media, eE1 alone was produced in the same mammalian cell expression system, however, total production yields are over 50-fold less (0.2 mg/L media). All the discoveries above suggested that apolipoproteins should be considered as an important co-factor of E1. For the eE1/apolipoproteins complex, approximately half of the mass is apolipoprotein and a quarter is glycan based on the mass spectrometry and AUC data.

E1 does not undergo an obvious conformational change at low pH. The sedimentation velocity experiment can be used to detect a subtle conformational change by testing both the pH effect and concentration effect for multiple samples. The result can verify whether a reversible self-association or mass action occurs around different pHs, as well as the affinity parameters at the end stage.

2 Characterization of eE1 in complex with antibodies

The ability of HCV E1 protein as a vaccine candidate has been controversial. E1 is recognized as a poor immunogen and less immunogenic than E2 [73]. The response induced by immunization of the HBV-HCV chimeric E1 was quantified, showing a much weaker response than E2 by a microparticle chemiluminescence immunoassay [74]. Compared to E2, there are much fewer E1 antibodies found in HCV patient samples and less characterized. Anti-E1 antibodies are rarely detected in significant quantities in patients [75].

However, there's few findings suggesting E1 can be a potential target for neutralizing antibodies induction. Firstly, E1 has a better sequence similarity among different genotypes than E2 and has more intergenotype cross-reactivity. Secondly, some anti-E1 antibodies have been reported to confirm the immunogenic function on E1. H-111, a human monoclonal antibody can weakly neutralize HCV genotype 1a, 1b, 2b, and 3a through a highly conserved epitope at the N-terminal (amino acid 192-211, YEVRNVSGVYH sequence) of E1 [76]. IGH-526 and IGH-505 are broadly neutralizing monoclonal antibodies targeting the amino acid 313-327 region [75]. Thirdly, the isolated anti-E1 antibodies were detected in chronically infected patient response which are effective for HCV clearance and vaccine design [77].

In conclusion, characterization of the interaction between E1 and antibodies may lead to a better understanding of the role of E1 during the HCV entry. In addition, the analysis of neutralizing properties of anti-E1 antibodies might be effective in vaccine strategies.

2.1 Generation of Monoclonal Antibodies

The mouse hybridoma antibody cell lines were generated through a collaboration with Dr. Arash Grakoui at Emory Vaccine Center. The overall procedure and timeline is shown (Table 3). At phase I, E1 (genotype 1b) 192-330 serum-free protein was used as the antigen

with the adjuvant to induce a robust immune response. One mouse was chosen out of ten with the best ELISA result of the pre- and after-immunization serum. At Phase II, the lymphocytes of the chosen mouse were collected, isolated, and fused with myeloma cells. The fused hybridoma cells were selected by a special media and diluted for the single cloned cell for continuous culture. The cell culture supernatant was collected with the ones shown the positive ELISA results with the antigen. At Phase III, the sub-cloned hybridoma cell lines were expanded to a 2 mL culture for further expansion.

2.2 Mapping the Antibody Binding Region by ELISA

To determine a broader range of the epitopes, the truncated versions of eE1 described in Section I were used in an ELISA. The hybridoma cell lines were expanded to a 0.5-liter culture and the supernatants were collected. Different supernatants were tested on nE1, cE1, eE1 192-303, eE1 192-311, eE1 192-330, eE1 192-342, and eE1 192-357 from genotypes 1a, 1b, and 2a.

Since the mouse antibodies were generated against the serum-free protein of eE1 192-330, it is not surprised that some of antibodies didn't interact with eE1 357 protein, such as 2F2 and 2F7, revealing the conformation differences between these two proteins. Interestingly, most of the antibodies can bind to the N-terminal of eE1, only 2F7 binds to C-terminal, leading to the result that N-terminal region of eE1 could be a good candidate for antibody recognition. All the antibodies interacting with eE1 192-330 can bind to a longer construct, eE1 192-342, as well, showing a similar conformation between these two proteins. However, eE1 192-342 might be relatively flexible or folded different near the antigen binding regions. Some monoclonal antibodies can cross-reactive with eE1 of different genotypes. 3D2 can bind to genotype 1a and 1b, while H-114 can interact with genotype 1b and 2a. Antibody 2F7 can interact with all three genotypes, suggesting its antigen binding region might be conserved among three genotypes.

In conclusion, the N-terminal of eE1 would be more immunogenic which could be useful

for therapeutic purposes.

2.3 Antibody Digestion and Fab Purification

Based on the results of binding region mapping on different anti-E1 antibodies, several were chosen for the downstream biochemical and structural studies. Around 20 hybridoma cell lines were expanded to larger scale cultures for purification. Most of the antibodies can be successfully purified and digested into antibody Fab fragments (Table 5).

However, a major impediment was that the production level varied from batch to batch, even the ones from the same starting culture. Hybridoma can be very heterogenous in population, grow at diverse rate or antibody production can be lost after prolonged time in culture usually after 10-20 passages. Hybridoma cell lines with poor growth rates were sub-cloned (2C1-1A, 2B12-D1, 2B12-G10, 2G9-G2 D1, 2F11-D1 D1, and 2B9-A5), by diluting into single cell and selecting the highest producing cell lines. However, the diluted sub-clones usually take few weeks to expand, which could result in missing the antibodies expressed during this time. To avoid this, multiple sub-cloned cultures can be chosen for expansion, for example, 2B12-D1 didn't produce any antibodies, whereas 2B12-G10 expressed much better.

It's hard to get the desired amounts of antibodies by the method discussed above, especially for crystallization trial. To solve this issue, a membrane flask was introduced for the alternative method to grow hybridoma cell lines, whose average expression level is 10 mg antibody per every 350 mL-membrane-flask.

Once the antibodies were purified, Papain digestion was performed to produce Fab fragments. The digestion time and production level of each antibody was shown in the Table 5. For different antibodies, the post-digestion purification method is quite different. The purified Fab fragments will be used as a potential co-crystallization scaffold.

2.4 Characterization of eE1/Fab Complex

Even if the full-length antibody can interact with eE1 by ELISA, however, for unknown reasons, the purified Fab fragment shows lower binding activity. Furthermore, certain Fab and Fc fragments cannot be distinguished clearly. We devised a further test by SEC to confirm the binding between eE1 and Fabs.

Antibody Fabs of 4E3, 2F2, 3C1, H114, 1D10, 2B12, 1D2, 2B12, and H111 were mixed with different truncated eE1 proteins with or without N-linked glycans at 1:1.2 molar ratio, followed by incubation on ice for one hour. The complex was loaded onto the superpose 6 column for characterization (Figure 18). The SEC profile of eE1 and Fab alone were used as controls. The elution volume of the complex should be smaller than either protein alone, due to the larger size of the complex. A complex with better homogeneity showed a symmetric, sharp peak on SEC. The excess amount of the antibody is added to for increasing complex formation, which can be visualized by SEC profile.

The initial binding test was with a 1:1 molar ratio of eE1 to the antibody, but some of the SEC profiles showed a much higher peak of the free antibody than expected, suggesting a different binding ratio. By changing the antibody amount and testing on SEC, a different ratio was found for 1D2 and 1D10 antibodies, revealing an approximate 1:2 binding of the protein to Fabs (Figure 19).

Even though some complexes form at the same binding ratio, the elution volume were quite different, suggesting the differences in the size or shape of the complexes (Figure 19). It would be interesting to probe the conformation of different complexes.

2.5 Crystallization Trials of eE1/Fab Complexes

X-ray crystallography is widely used for identifying the atomic and molecular information of a protein, as well as the contact information for protein and antibody complex. A high-resolution structure will provide new directions to understand the molecular mechanisms of E1 function.

Antibodies can be a crystallization chaperone to aid the structural determination of the flexible proteins [78]. For flexible proteins, an antibody can trap it in a specific conformation, increasing homogeneity and the possibility for crystal formation. For the solvent-exposed loops, some antibodies can assist in the formation of crystal lattice by increasing the hydrophilic surface area of the binding complex [79]. Mass spectrometry result shows that eE1 is under different glycosylation states and different conformations. Antibody may "lock" eE1 at a specific conformation, increasing the chances of forming crystals.

The Fab fragment is identified as a better scaffold than the full-length antibody. The small size of Fab would eliminate the flexibility around the antibody binding region, which can make the crystals packing more spacious and rigid. An early use of antibody Fab in crystallography published in 1990. HIV capsid p24 was co-crystallized with Fab reaching to 2.7 Å resolution [80]. Another advantage of using Fab fragment in crystallography is to help determine the phase. For model-based phase determination, the approach is to pursue molecular replacement using a library of Fab structure, because the overall structure of Fabs are very similar. The high-resolution structure of nE1 can also be a phase determination tool for molecular replacement method [26]. Overall, it might facilitate the crystal formation of eE1 by co-crystallization with anti-E1 Fab fragments.

Complexes consisting of both fully-glycosylated and deglycosylated eE1 in different truncations with different antibody. Fabs were purified by SEC and screened for crystallization using commercial kits at two temperatures (Table 6). Among the different combinations, two complexes successfully formed crystals from the 96-well initial screening

on sitting drop plate.

The first one is deglycosylated Con1 eE1 192-352 linker protein with H-111 Fab complexed in 20 °C at 7-10 mg/mL. The crystallization solution consists of 4% v/v Tacsimate pH 4.0 and 12% w/v Polyethylene glycol 3,350. The 20 μm-sized small football-shaped crystals started form after 20 days and slowly grew to the full-size in 60 days (Figure 20A). However, the growth time was too long which can cause the degradation of the protein. Moreover, the crystals from this condition were difficult to reproduce.

The second one is Con1 E1 192-357 fully glycosylated protein with 2B12-G10 Fab complexed in 20 °C at around 12 mg/mL. The crystallization solution consists of 0.1 M ammonium sulfate and 12% w/v Polyethylene glycol 3,350. The 400 μm-sized hexagonal prisms-shaped crystals formed overnight and grew to maximum size in the following three days (Figure 20B). One crystal was directly analyzed on an X-ray home source at Center for Advanced Biotechnology and Medicine (CABM) at a 3.5 Å resolution dataset. Data processing and unit cell size suggested the presence of antibody alone, implying that the complex dissociated in this crystallization condition. These hexagonal crystals were covered by cloudy precipitation, which might be eE1 protein. The pH value of this crystallization condition is about 5.0 which may disrupt the complex. To test this hypothesis, the complex was analyzed by SEC with low-pH elution buffer, showing the complex was separated into two peaks (Figure 21). Further analysis revealed that Fabs failed to complex with eE1 below pH 5.0. Further crystallization trials of eE1 and antibody complex are ongoing.

2.6 Discussion

The reasons why eE1 is characterized as a weak immunogenic protein could be due to the presence of glycans and apolipoproteins that cover the eE1 surface. Glycans can influence the immunogenicity of the protein by inhibiting the antigenic conformation or exposure of antigenic site [73]. In addition, glycans can alter the proteolytic susceptibility of proteins, which leads to the surface charge change of the protein. A study has shown that by the

mutagenesis on E1 protein glycosylation site, the immunogenetic property has changed using a specific ELISA measurement on intramuscular and intraepidermal injection to BALB/c mice [73]. The apolipoprotein can "shield" the antibody binding for similar reasons.

A new batch of anti-E1 antibodies are being generated using Con1 eE1 192-357 protein as the antigen, since some of the previous hybridomas do not grow well or antibody binding was poor. The neutralizing antibodies, especially the broadly neutralizing antibodies, can be used for therapeutics treatment and vaccine design. The anti-E1 antibodies need to be assayed HCV neutralization followed by epitope mapping to identify areas of vulnerability on eE1. The most immunogenic epitope can be used for future vaccine design.

3 Characterization of E2 the Interaction between E2 and Cell Surface Receptor CD81

The function of HCV E2 glycoprotein is better defined than E1. During the HCV entry, E2 plays a major role in cell surface receptor complex binding. E2 mediates virus entry through interaction with cell surface receptors and is highly immunogenic. Numerous neutralizing antibodies have been founded against E2. E2-specific antibodies derived from human sera can neutralize HCVcc in vitro [81]. E2 has a selective advantage by recognizing the antibodies target specific region [82].

It has been a challenging task for years to express HCV E2 protein, because it's heavily glycosylated, flexible and contains several disulfide bonds. The similar strategy of mammalian cell expression method was used to produce the E2 full-length ectodomain seeking for more structural information.

CD81 was identified in 1990 as a surface protein expressed on most human cells [83]. CD81 belongs to transmembrane 4 superfamily with the function as signal transduction, cell regulation, and immune cells differentiation [84]. This tetraspanin protein consists of four transmembrane segments with the linkers in between, a short extracellular loop (SEL), a large extracellular loop (LEL), and a short intracellular loop. The crystal structure of human CD81-LEL reveals a mushroom-like structure in a homodimeric form [85] (Figure 22).

The crystal structure of human CD81-LEL reported that Thr163 and Phe186 residues on human CD81 were crucial for the CD81 E2 interaction by mutagenesis analysis [86]. In addition, the interaction depends on the integrity of the two disulfide bonds bridge and the dimerization of CD81-LEL [87] [88].

CD81 is the first identified HCV receptor in 1998 with the function of directly interacting with HCV E2. CD81-specific antibody can block the HCV infection, suggesting

that CD81 can mediate the post attachment of HCV entry and cause the conformational change on E2. In addition, several neutralizing antibodies against E2 can specifically block E2/CD81 interaction [89]. The interaction regions were narrowed to amino acid 412-423, 432-447, and 528-535 on E2, named as CD81 binding loop, by antibody blocking assay [90]. Moreover, CD81-LEL can stabilize the E2 conformation at low-pH, taking advantage of the flexibility of the CD81 binding loop [37]. However, it is unclear about the E2 and CD81 interaction in details.

The crystal structure of H77 eE2 core protein with a Fab fragment reveals the interaction region belongs to the CD81 binding loop. Phe537 and Lys539 residues on CD81 binding loop were flipped into the hydrophobic core, whereas in the J6 eE2 core structure, the CD81 binding loop region is disordered and solvent exposed (Figure 23) [23] [25]. In both HCV pseudoparticles and cell culture-derived HCV particles, the secondary structure of CD81 binding loop is dependent on the binding of different antibodies [91]. CD81 binding requires a correctly-folded E2, but there's no conformational information on CD81 binding loop [92].

To get a better understanding of the E2 and CD81 interaction, an atomic resolution structure was needed, which might reveal an unpredictable secondary structure of the CD81 binding loop. The detailed structural information can be used in drug design by discovering a molecular as an inhibitor to block the interaction site. A high-resolution structure will provide the new directions to understand the molecular mechanisms of antibody-mediated protein and receptor interaction.

3.1 Full-length eE2 Expression and Purification

eE2 has an N-terminal ectodomain followed by an α-helical stem and a carboxyl-terminal transmembrane helix. (Figure 2A). E2 has 9-11 glycosylation sites depending on genotype and 18 cysteines for disulfide bonds which are absolutely conserved.

The full-length eE2 (amino acid 384-656) was expressed in HEK293S GnTI^{-} cell line

with lentivirus infection method followed by purification, which can reach to the yield at 20 mg per liter of the culture media for both H77 and J6 genotypes.

3.2 ΔHVR1 eE2 Expression and Purification

The hypervariable region (HVR) is a genome region where the base pairs are made of a variable number of repeated sequences, which is usually exposed or flexible.

Neither of the published structure has included the N-terminal of eE2, especially the HVR1 (amino acid 384-410) [93]. Hydrogen-deuterium exchange and limited proteolysis was used to probe the first 72 amino acids of E2, including both HVR1 and HVR2, showing HVR1 is a flexible and solvent exposed region with several glycosylation sites [23].

Genotype 1a and 2a of ΔHVR1 eE2 protein were expressed for characterization on the function of HVR1 by comparing to the properties of full-length eE2. HVR1 is reported to be an important epitope for SRB1, CD81, and neutralizing antibodies binding [94]. The ΔHVR1 eE2 (amino acid 411-656) was expressed in HEK293S GnTI^{-} cell line with lentivirus infection method followed by purification, which can reach to the yield at 20 mg per liter of the culture media.

3.3 Oligomeric Study of eE2

The disulfide-linked high oligomers can be shown on the Coomassie-stained SDS-PAGE with higher molecular weight bands at non-reducing condition, whereas a single band with the reducing reagent (Figure 24A). The SEC profile of eE2 shows mainly two peaks (Figure 24B). The eE2 dimer elutes earlier followed by a sharp symmetric peak of the eE2 monomer. From the SDS-PAGE and SEC result, approximately 20% of eE2 species is at the dimeric form, but the majority is monomer.

To enhance the homogeneity of eE2 for the following biophysical and structural study,

the monomer, as the dominant species of eE2, was isolated and collected. In conclusion, both full-length eE2 and ΔHVR1 eE2 are monomeric in solutions which confirms the previous finding [23].

3.4 Expression and Purification of Human and Tamarin CD81-LEL

HCV can only infect humans and chimpanzees [95]. Mouse CD81 cannot interact with HCV particles from the serum [89]. However, tamarin CD81 can interact with HCV E2 with an approximate 10-fold higher binding affinity than human CD81 [96]. Tamarin, as a New World monkey and is a suitable animal model for many human viruses. In addition, tamarin CD81 can substitute for human CD81 during HCV entry [96]. CD81-LEL is highly conserved between differences species, with only five amino acid differences of human and tamarin (Figure 25).

CD81-LEL has four cysteine residues to form the disulfide bonds and no N-linked glycosylation sites [90]. Both human and tamarin CD81 were expressed in HEK293T cell line with lentivirus infection method followed by purification, which can reach to the yield at 10 mg per liter of the culture media for both species. CD81-LEL expressed in mammalian cells is proper-folded and soluble comparing a similar construct produced in bacteria (Figure 26).

3.5 Interaction between E2 and CD81-LEL

The crystal structure of human CD81-LEL shows an antiparallel dimer, whereas E2 core structure is at a monomeric form in solution [85] [23]. It is unclear how a CD81-LEL dimer can recognize the monomeric E2. SEC and Isothermal titration calorimetry (ITC) methods were used to study the stoichiometry of E2/CD81-LEL interaction.

Different molar ratios (1:1, 2:1, and 1:2) of the purified fully-glycosylated full-length eE2 and CD81-LEL proteins were mixed together followed by SEC analysis. E2 and CD81-LEL showed heterogeneous binding for all different ratios of mixture. Two major peaks on the

SEC were collected and analyzed by SDS-PAGE, revealing two different species. It's clear to visualize the E2/CD81 complex and E2 alone, which in theory should have another species of CD81-LEL alone. However, the UV absorbance at 280 nm for CD81-LEL was relatively low due to the presence of a single Tyr residue, making it difficult to detect using standard protein chromatography. None of different E2:CD81-LEL ratios allowed for the formation of a single complex (Figure 27).

For a more quantitative study of the protein-protein interaction we employed isothermal titration calorimetry (ITC). ITC directly measures the heat releasing and absorbing associated with a chemical reaction triggered by the mixing of two components. The binding constant (K_d), stoichiometry (n), and enthalpy of binding (ΔH) can be determined, as well as some other thermodynamic parameters. ITC does not require modification or immobilization the protein samples. However, ITC does require a larger quantity of samples compared to other affinity measurement techniques, such as surface plasmon resonance.

The binding affinity was measured of both human and tamarin CD81-LEL to HCV E2 protein. Tamarin CD81-LEl has a 5-fold tighter affinity than human CD81-LEL, consistent with previous qualitative methods done in tissue culture media [96] (Figure 28). The binding ratio of E2 to CD81-LEL is around 0.5 for both species, which suggests that a portion of E2 may interact with CD81-LEL dimer. The same experiment was repeated multiple times with a different binding ratio number every time, but a similar dissociation constant within the error. The ITC result of the binding ratio didn't match our previous observation using SEC method and couldn't get any theoretical evidence to support. One hypothesis could be that the sample we purified is partially active, for example, if the binding is ratio is o.7, which means a 1:1 binding with 30% inactive form of eE2.

In conclusion, tamarin CD81-LEL can interact with eE2 by a higher affinity than human CD81-LEL in binding. Tamarin CD81 can be a candidate for the following biophysical and structural study.

3.6 Antibody-mediated Receptor Binding

To study the CD81 and E2 interaction, H77 eE2 with CD81 complex was characterized using SEC by the same method as J6 eE2. The SEC of the H77 eE2 and human CD81-LEL complex was much more complicated than J6, showing multiple peaks overlapping on each other. Coomassie-stained SDS-PAGE was not able to identify the components of each peak because different peaks cannot be separated to different fractions of the column elution.

Anti-E2 antibody 2A12 Fab was co-crystallized with eE2 core in the high-resolution structure [23]. In this way, 2A12 should have stabilized E2 by changing from disordered to an ordered conformation. The binding site of 2A12 is on the C-terminal and far from the CD81 binding loop, which should not block the CD81 interaction.

H77 full-length eE2 was first complexed with 2A12 Fab and then human CD81 with 1:1:1 molar ratio followed by SEC characterization. On the chromatography, a sharp symmetric peak was at a smaller elution volume prior to the elution volume of E2/Fab complex, identified as the E2/Fab/CD81-LEL complex. By overlapping the chromatography of E2/CD81-LEL complex and E2/Fab/CD81-LEL complex, it is clear that antibody can help with homogeneity and complex stability (Figure 29).

Interestingly, a non-neutralizing antibody can facilitate the formation of E2/CD81 complex. This is a striking observation that may have implication for viral infection but needs more work to confirm this observation.

3.7 Crystallization Trials of full-length eE2 with CD81-LEL

Deglycosylated J6 full-length eE2 was complexed with 2A12 Fab followed by mixing with human or tamarin CD81. In this way, the antibody fragments would serve as crystallization chaperones to aid the structural determination and especially conformational homogeneity.

The initial screening is performed using a series of commercial, preformulated crystallization reagents by sitting drop vapor diffusion method [39]. For each condition, three different protein samples were analyzed. In the first sub-well, eE2/Fab/CD81-LEL complex was applied, while eE2/Fab and CD81 alone serve as controls. The expected result is crystals formed in the first sub-well and no crystals on the last two sub-wells. However, no crystals were observed within 6 weeks after the initial screening with the complex of full-length eE2 with 2A12 Fab and human CD81-LEL.

Glycans can assist in the protein folding and crystal packing. The crystal structure of HIV gp120 with homogeneous oligomannose glycans was determined, revealing the glycoprotein is reactive to a glycan-mediated antibody [97] [98]. Since N-linked glycosylations can stabilize the protein fold of the protein and their glycan electron density can be visualized in detailed structure, we decided to attempt crystallization with fully glycosylated eE2 [99]. Thus, the fully-glycosylated eE2 was used for crystallization and crystals were found in three conditions. Thus, the fully-glycosylated eE2 was used for crystallization and crystals were found in three conditions (Figure 30) (Table 7).

3.8 Crystallization Trial of ΔHVR1 eE2 with CD81-LEL

By making a deletion of the flexible loop and solvent-exposed hydrophobic residues, the stability of the protein may increase crystal formation. ΔHVR1 eE2 was complexed with 2A12 Fab and CD81-LEL for crystallization screening.

No crystals were found from ΔHVR1 eE2 with 2A12 Fab and human CD81-LEL observing within 6 weeks, which might due to the low binding affinity between human CD81 and E2.

For ΔHVR1 eE2 with 2A12 Fab and tamarin CD81-LEL, within 3 days after setting up, the complex crystals were formed in 11 different conditions (Table 8). Interestingly, the crystallization conditions are usually with 0-0.2 M salt and pH 4-6 with 10-20% PEG

solution. The images of the crystals from different conditions are shown (Figure 31). The size of some initial crystals can reach to 100 μm in the longest dimension (Figure 31).

ΔHVR1 eE2 crystals were better in both shape and size than the ones of full-length eE2. The following optimization will focus on the fully-glycosylated J6 ΔHVR1 eE2 with 2A12 Fab and tamarin CD81-LEL crystals.

3.9 Optimization and Additive Screening on Fully-glycosylated ΔHVR1 eE2 with 2A12 Fab and Tamarin CD81-LEL Crystals

Crystal optimization is done by hanging drop diffusion method using 24-well plate with a gradient of sodium acetate trihydrate pH 4.6 and PEG 3,350. The crystals grew to a size of 200 μm in a football shape and were confirmed as a E2/Fab/CD81 complex by the SDS-PAGE (Figure 32).

To improve the size and shape of the crystals, additive screening was applied using a commercial kit with the initial condition of 0.2 M sodium acetate trihydrate pH 4.6 and 14% (w/v) PEG 3,350. A list of additive conditions and crystals images are shown (Figure 33), however the crystals weren't improved in size and shape as expected.

3.10 Data Collection and Modeling of the E2-CD81 Interaction

Crystals were cryo-protected using reservoir solution with 25% (v/v) 2-methyl-2,4-pentanediol and flash cooled in liquid nitrogen. The crystal with 4.3 Å resolution belongs to space group $P2_12_12_1$ with cell parameters a= 77.78 Å, b= 128.1 Å, c= 223.4 Å with all angles 90 °. Phases were determined by the molecular replacement method using PHENIX with eE2 core (PDB ID: 4WEB) and human CD81-LEL (PDB ID: 1G8Q). COOT was used for refinement followed by fitting the CD81-LEL structure into the density map. After rounds of further refinement, the final model was built with a resolution of 4.3 Å (Figure 34).

Overall, the complex formed a twisted-belt-like structure (Figure 35). The dimer of tamarin CD81-LEL was interacted with two E2s on each side. E2 was stabilized by Fab fragments on the opposite side of the CD81 binding region. Phe537 residue on E2 is identified on the CD81 binding loop [25], while Phe186 residue on human CD81 plays an important role on E2 binding by mutagenesis experiment [90].

In our preliminary model, E2 Phe537 and CD81 Phe186 residues are at the interface. Better resolution for the complex is needed to confirm the interaction.

3.11 Discussion

One interesting observation is that neither ITC nor SEC result can accommodate the 1:1 ratio of binding model on E2/CD81 interaction. The stoichiometry (n) is less than 1 by ITC, suggesting a portion of E2 was not active for CD81 interaction. Fully glycosylated full-length eE2 was used on the binding assays, however, glycans might have an influence on the E2/CD81 binding. Mutagenesis of different glycosylation sites on E2 could decrease, increase, or have no effect on the E2/CD81 binding [100]. It overstated that by removing of the glycans on Asn417 and Asn32 residues of E2, CD81 binding loop could be overexposed to enhance the interaction [100].

To make the interaction more detectable by ITC, a higher concentration of the sample or the removal of glycans can be used in exaggerating the signal. By enhancing CD81 and E2 binding to make it a “tight and rigid” complex, the possibility of crystal formation can be increased as well.

Most of the crystals formed in low-pH crystallization reagent, suggesting the conformation of E2 and CD81 complex is more stable at low-pH. The complex can be purified and formed at low-pH in order to get a better result in crystallization trial. The further optimization of the crystals is undergoing.

4 Characterization of cell surface receptor SRB1

SRB1 is a cell surface glycoprotein that can uptake cholesterol from circulating lipoproteins and deliver it to the liver for degradation. SRB1 can bind to HDL and the oxidized form of LDL followed by delivering to steroidogenic tissues and liver cells [101]. SRB1 is reported to be overexpressed in many human cancers and most tumor cells, including prostate, colorectal, breast and ovarian cancers [102]. SRB1 was suggested to be very prominent therapeutic agent [103], as well as a potential cancer biomarker [104]. SRB1 was identified as an HCV receptor in 2002 and has been reported to interact directly with HCV E2 protein [30]. SRB1 wasn't expressed much in the majority of the human cells [105], which benefits SRB1 to be a drug target in cancer therapy or HCV treatment [106].

4.1 Construct Design of SRB1 Ectodomain (eSRB1)

SRB1 is composed of 509 amino acids, with a molecular weight of approximately 82 kDa due to the 11 glycosylation sites on the ectodomain [107]. It consists of two transmembrane helices at both N-terminal and C-terminal of the large ectodomain.

SRB1 belong to CD36 superfamily which contains three members, SRB1, lysosomal integral membrane protein type 2 (LIMP-2) and CD36 [108]. Interestingly, the crystal structure of LIMP-2 has been reported to contain a helical bundle on ligand binding region and a large cavity traversing the entire length of the molecule. By mutagenesis on SRB1 residues which predicted to be in the cavity, the researchers proposed that SRB1 could contain a similar tunnel conformation which is responsible for cholesterol or cholesterol ester transfer [109].

Based on the crystallization construct of LIMP-2, the SRB1 ectodomain construct was designed in a similar region followed gene synthesis and fused into pJG vector to be ready for lentivirus transfection.

4.2 Expression and Purification of eSRB1

Due to the post-translational modifications on SRB1, mechanistic and structural studies have been hindered by lacking method to produce the SRB1 proteins in good quantity and quality.

The eSRB1 (amino acid 38-431) was expressed in HEK293S GnTI^{-} cell line with lentivirus infection method followed by purification achieving yields of about 40 mg per liter of the culture media. The purified monomeric form of eSRB1 is properly folded and soluble as determined by SEC (Figure 36A).

4.3 Biophysical Analysis of eSRB1

Analysis the antibody interaction is an easy method to test the whether the purified eSRB1 was functional. A human monoclonal SRB1 antibody, mAb16-71, is effective in blocking HCV dissemination. eSRB1 produced in our system is recognized by mAb16-71 antibody by ELISA, confirming the proper folding of eSRB1 (Figure 36B).

4.4 Interaction between HCV E2 and SRB1

The N-terminal of E2 can associate with SRB1, especially the hypervariable region (HVR1) [110]. It is reported that SRB1 binding to E2 could facilitate the following CD81 binding [111]. In this model, HCV enters the hepatocytes in a coordinated fashion, beginning with the initial binding to SRB1 and triggers the conformational changes on E2, which in turn can bind to the cell surface receptor CD81 [112].

The interaction between E2 and CD81 was determined, but we couldn't detect any direct association between HCV eE2 and eSRB1. One reason could be that the interaction required the transmembrane region of either protein. Yet, there's no evidence from our previous results to support the successive E2-SRB1-CD81 binding model.

The underlying mechanism regarding HCV binding to SRB1 is still unclear. Due to the crucial role of SRB1 plays in HCV entry, a better understanding of the functional and conformational insights is needed.

4.5 Discussion

The sequence similarity of LIMP-2 and SRB1 is 34.56% which could be hard to use the LIMP-2 structure as a model for SRB1. With no common binding ligands reported between LIMP-2 and SRB1, it is not reliable to propose any conformational or structural insights on the SRB1 and E2 binding interface.

A small molecule compound, ITX5061, was the first drug used to inhibit HDL lipid transfer which has the functional of blocking E2 binding to SRB1 [105]. In addition to the prominent role of SRB1 in cancer research as a potential drug candidate, SRB1 can be used to design new therapeutics to efficiently block HCV infection.

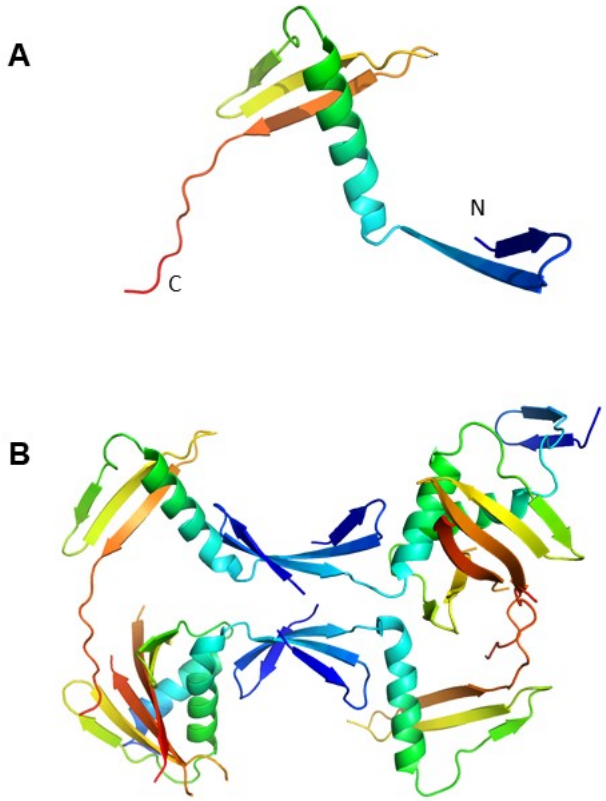

Figure 1: Crystal Structure of N-terminal Domain of E1 (nE1) in Complex with Antibody

(A) The crystal structure of nE1 (amino acid 192-270) monomer (PDB ID: 4UOI).
(B) The asymmetric unit is shown with six molecules of nE1.

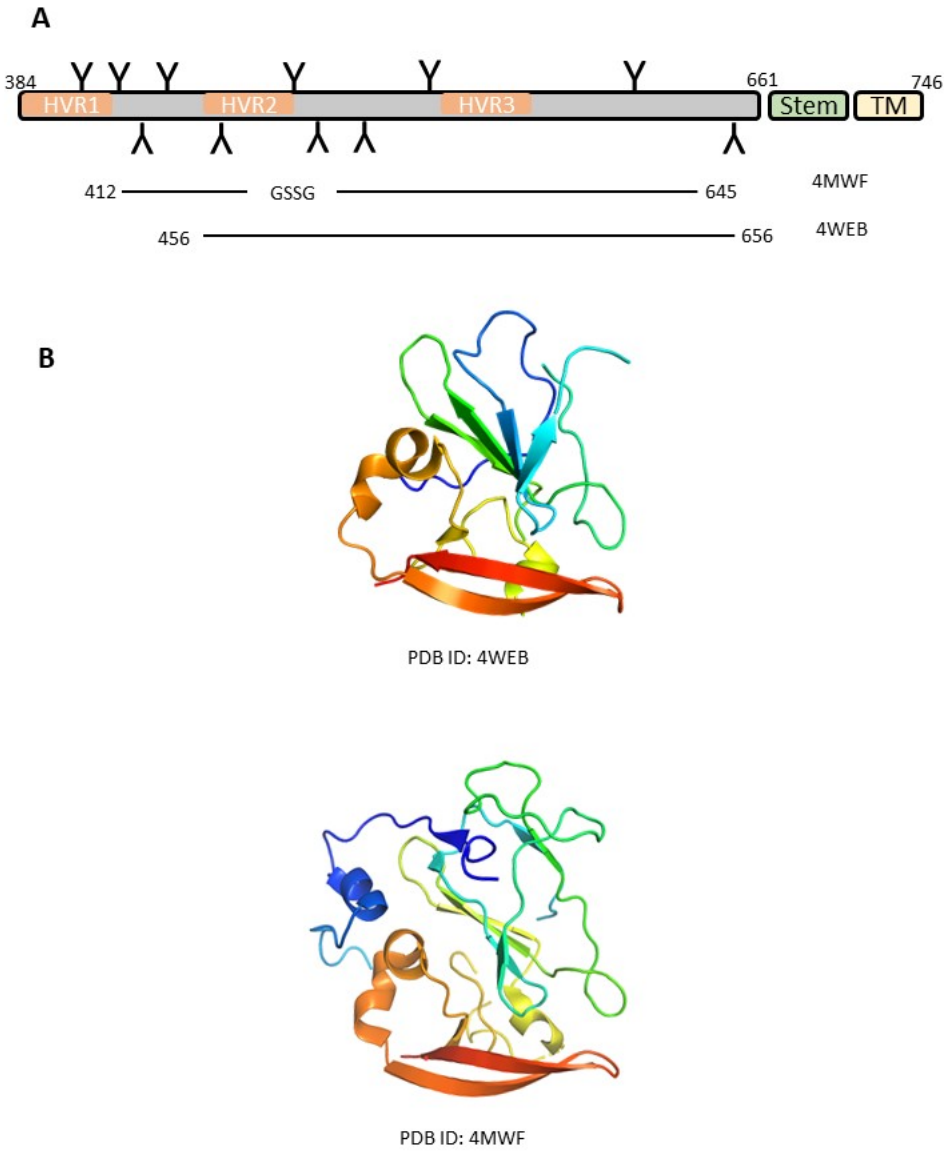

Figure 2: Crystal Structure of E2 Core in Complex with Antibody

(A) Linear diagram of the domain organization of E2. The locations of glycosylation sites are shown in "Y" figures, Stem is in green, transmembrane region is in yellow, and the three HVR (amino acid 384-410, 454-491, and 586-596) are shown in red. The crystal constructs are shown with PDB IDs

(B) Ribbon representation of E2 core structures (PDB ID: 4WEB and 4MWF).

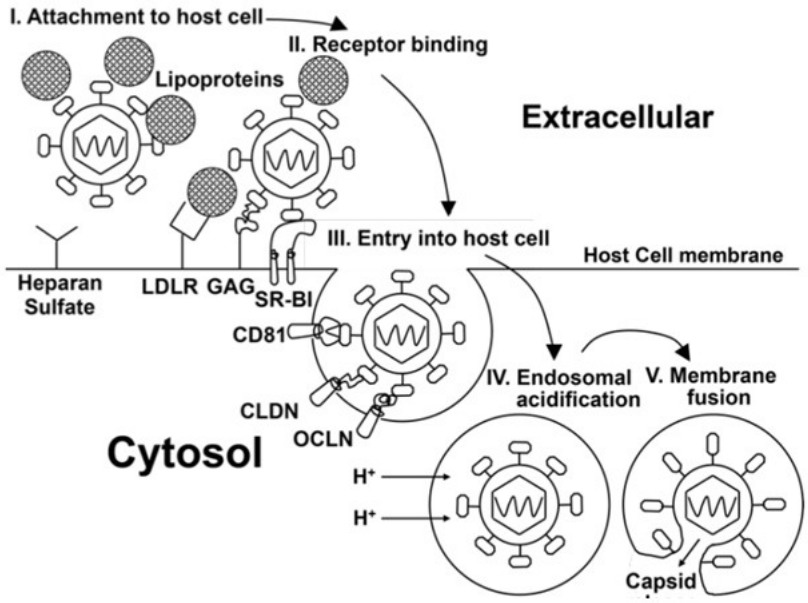

Figure 3: The Model of HCV Entry

I. Initial attachment to host cell by interacting with LDLR and GAG.
II. Receptors and cell entry factors binding, including SRB1, CD81, OCLN, and CLDN
III. Entry to host cell
IV. Low-pH triggered conformational and oligomeric state change
V. Membrane fusion

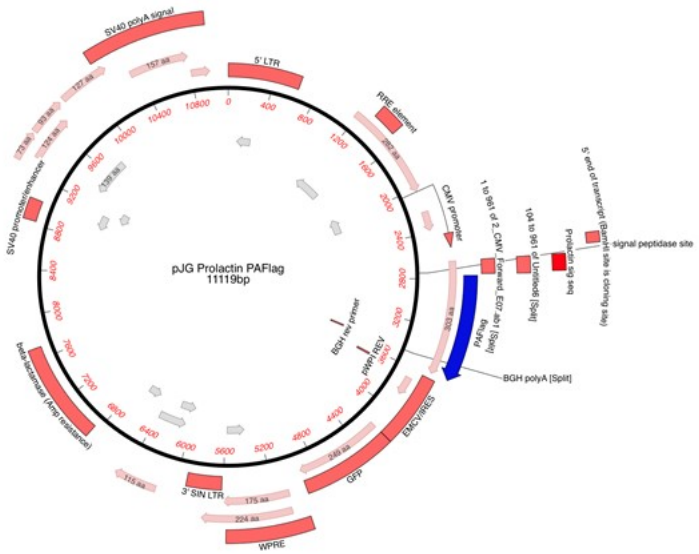

Figure 4: The Map of pJG Vector

The pJG vector consists of a cytomegalovirus (CMV) promotor, a rev response element, a woodchuck hepatitis promotor response element and a prolactin signal sequence to promote secretion and proper trafficking. The sequence of target protein is followed by a C-terminal 3XFlag tags.

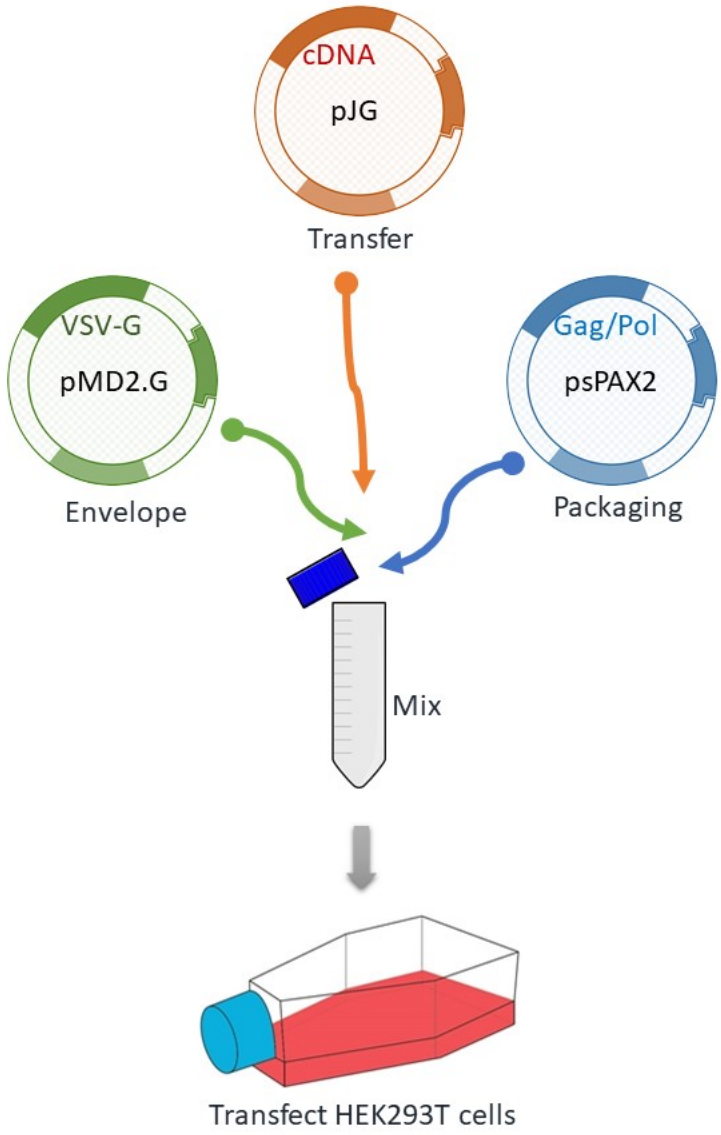

Figure 5: The Production Infectious Transgenic Lentivirus

Three plasmids are transfected into HEK293T cells, including a transfer plasmid (pJG), a packaging plasmid (psPAX2) and a envelope plasmid (pMD2.G).

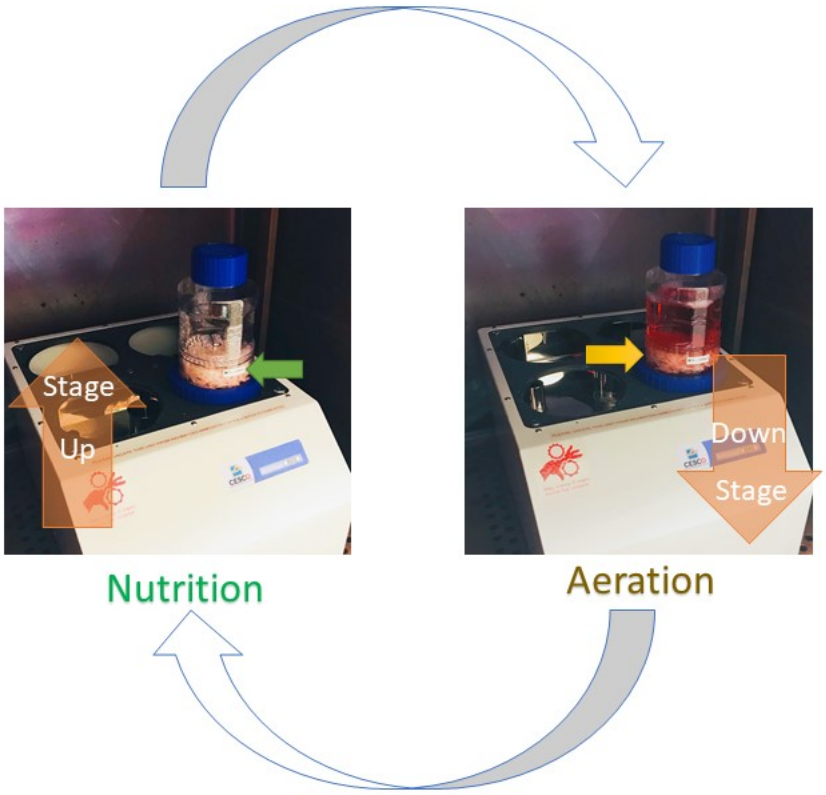

Figure 6: Two-Step Feeding Strategy on BelloStage

BelloStage can hold 4 bioreactors. The time for nutrition and aeration is adjustable. When the stage descends to the bottom, the cells are exposed to the air for aeration. When the stage rises to the top, the cells are in direct contact with the media to uptake nutrients.

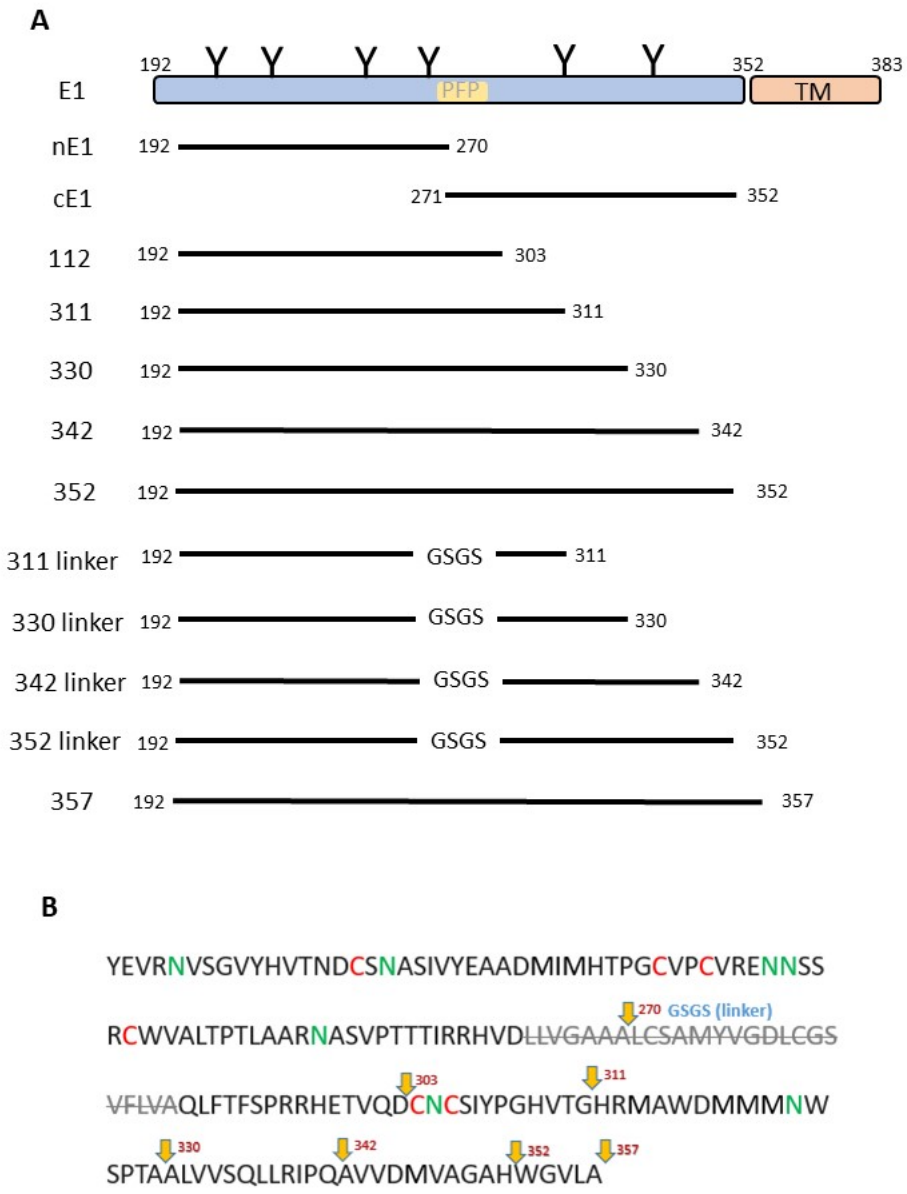

Figure 7: The Domain Organization and the Construct Design on E1

(A) Linear diagram of E1 glycoprotein. The tested E1 constructs are shown below the diagram. The location of glycosylation sites are shown in "Y" shape, predicted fusion peptide is shown in orange (amino acid 262-290), and transmembrane region on red.
(B) The sequence of Con1 eE1. The possible glycosylation sites are shown in green and the cystines were shown in red. Yellow arrows are the ends of each construct and the deletion was shown in grey.

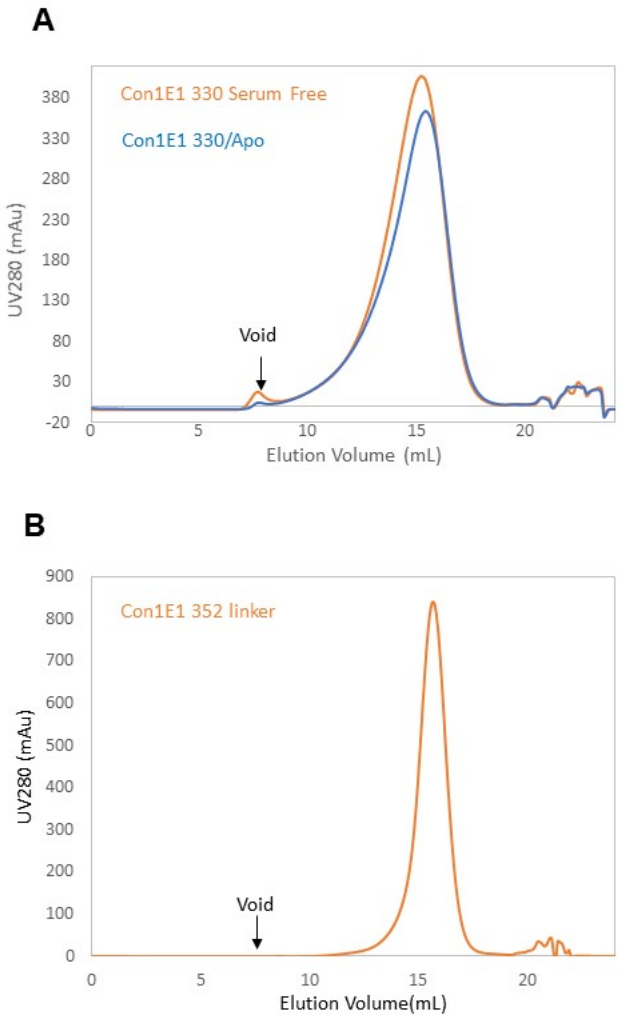

Figure 8: The SEC of Different Truncated eE1

(A) The profile of Con1E1 330 with apolipoprotein complex shown in blue, whereas Con1E1 330 serum free protein shown in red. Both of them have some aggregation at the void volume of Superose 6 column.

(B) The Con1E1 352 linker protein with apolipoproteins shows a nice sharp peak on Superose 6 column.

The elution buffer for SEC is 20 mM HEPES pH 7.5 with 100 mM NaCl.

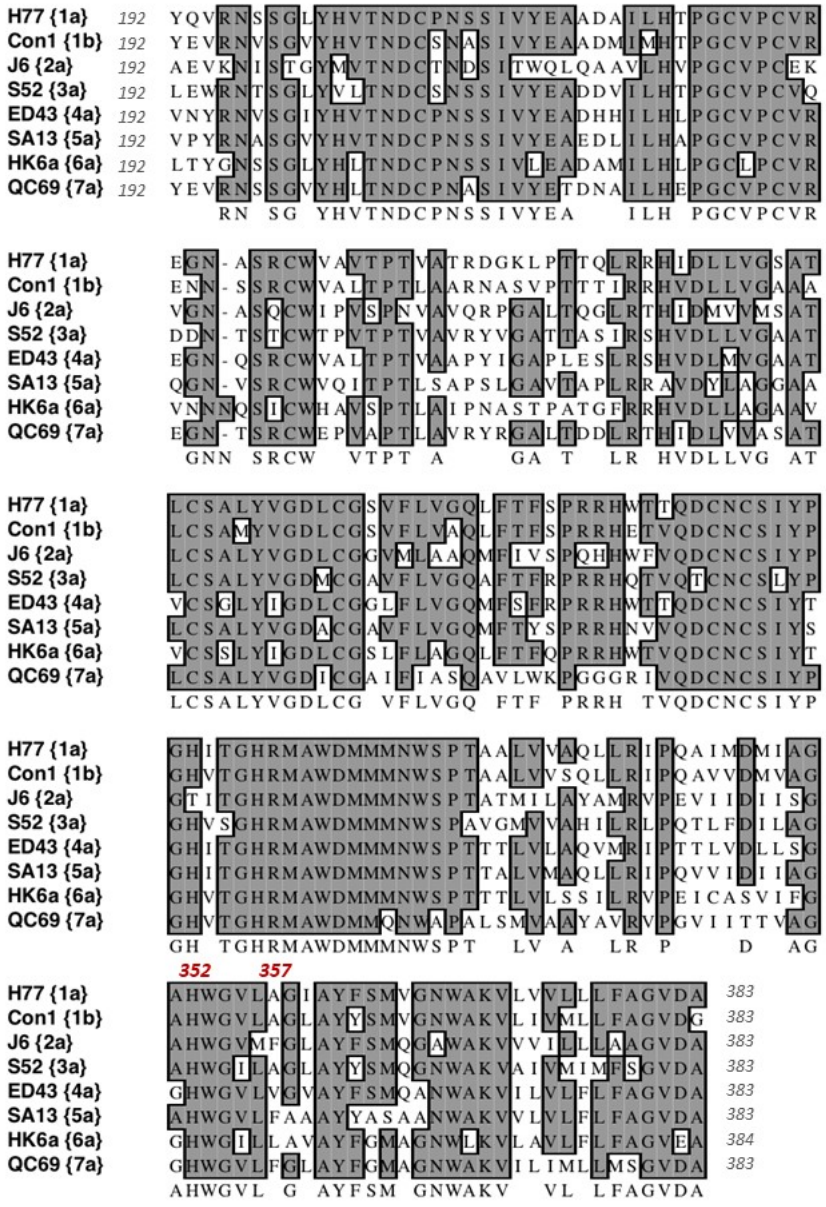

Figure 9: E1 Sequence Alignment of Different Genotypes

E1 (genotype 1-7) is aligned by ClustalW. The grey box shows the conserved residues. The His352 and Ala357 residues are labeled in red. eE1 352-356 region is highly conserved among all the genotypes.

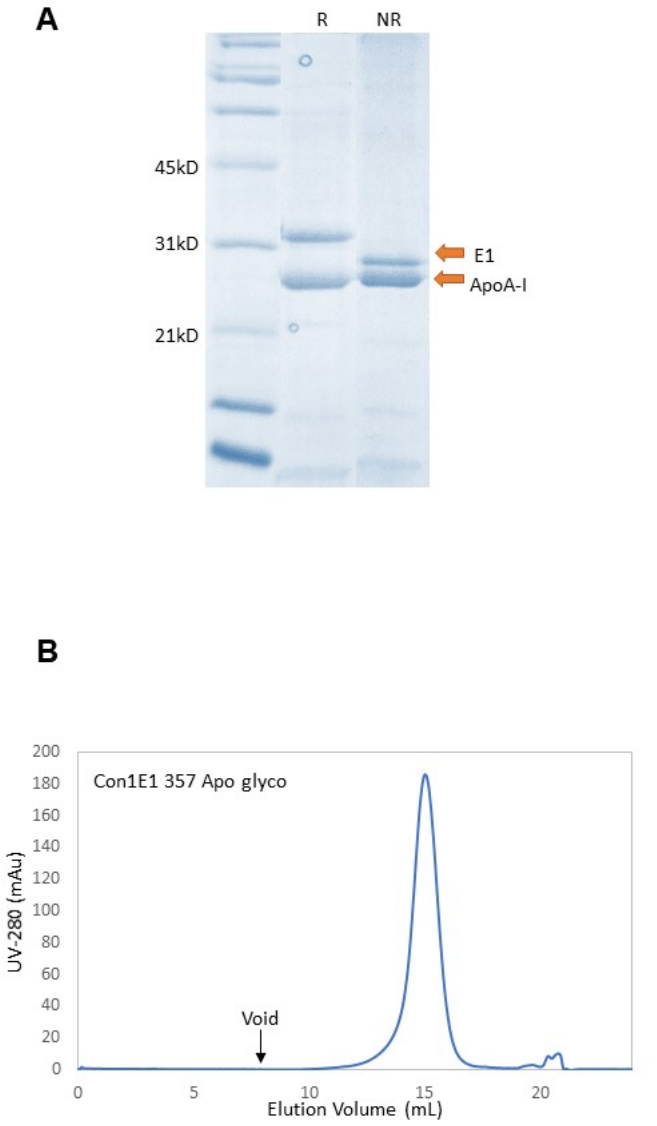

Figure 10: The SDS-PAGE the SEC Profile of eE1 357

(A) SEC profile on eE1 357 is with reduing (R) and non-reducing (NR) conditions. The two major bands by SDS-PAGE on Con1 eE1 357 protein are identified by mass spectrometry as E1 and bovine ApoA-I.

(B) The SEC of Con1 eE1 357/apolipoproteins shows a single sharp peak. The elution buffer for SEC is 20 mM HEPES pH 7.5 with 100 mM NaCl.

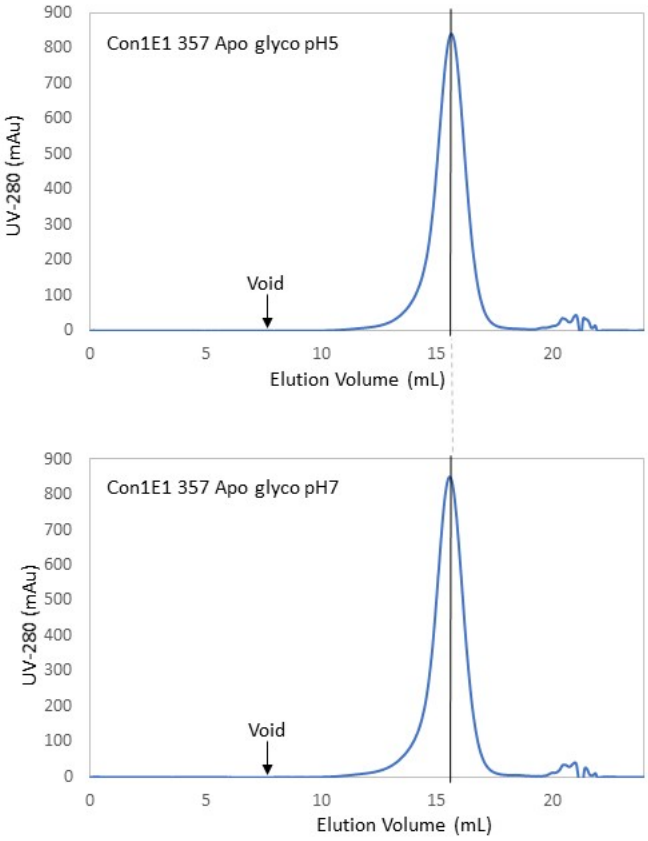

Figure 11: The SEC of eE1/Apolipoproteins at Different pHs

eE 357 is eluted by different pH buffers on SEC. The elution volume and size distribution of the protein at pH 5.0 and pH 7.0 is very close. The elution buffer for SEC is 20 mM sodium phosphate (pH 5.0 or 7.0) with 100 mM NaCl.

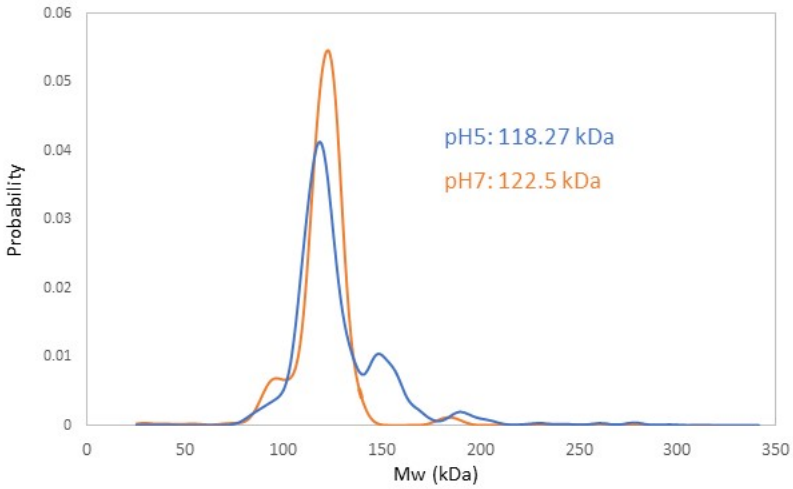

E1	Apo-AI	Apo-AII
28.35 kDa	28.43 kDa	8.5 kDa

3(AI)+E1+AII	3(E1)+AI+AII	*2(E1)+2(AI)+AII*
122.14 kDa	121.98 kDa	*122.06 kDa*

Figure 12: AUC Profile on eE1 at Different pHs

The mass distribution of eE1 at pH 5 is shown in blue and pH 7 is in orange. eE1/apolipoproteins complex is undergoing a subtle conformational change at low pH, showing only 3 kDa mass difference. Based on our calculation, E1 and ApoA-I might form a dimer complex along with ApoA-II. At pH 5.0, a small amount of protein might be able to form a trimer complex, shown a small peak around 150 kDa.

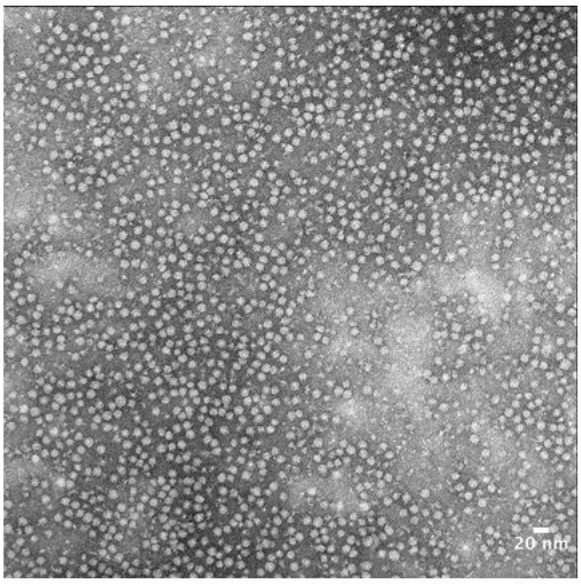

Figure 13: The Negative-stain of eE1 in Complex with Apolipoproteins

The size of the fully-glycosylated Con1 eE1 357 particles is around 10-14 nm in a global shape using UranylLess as a stain reagent.

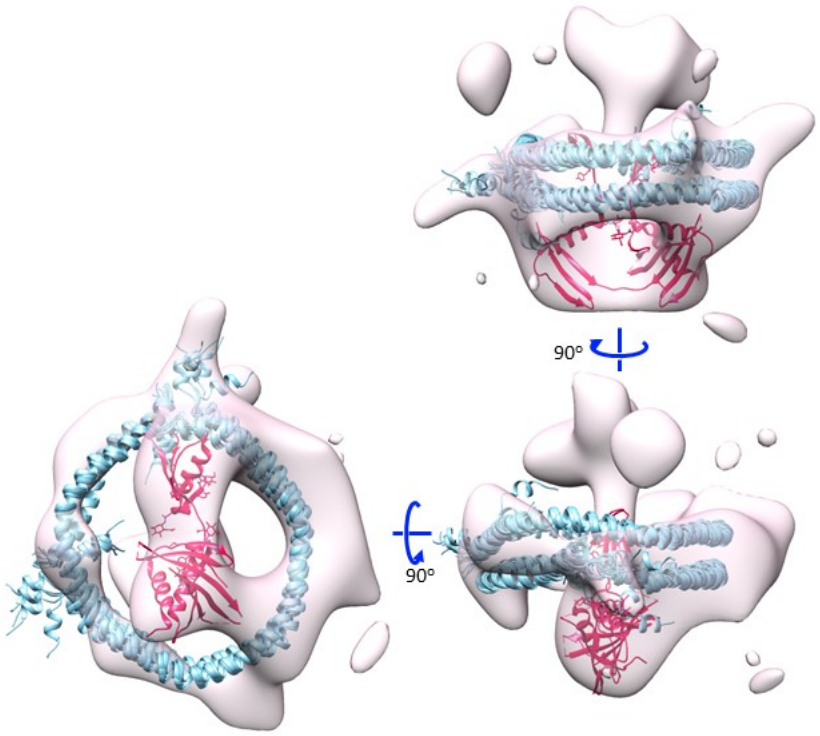

Figure 14: The Bean-like EM structure of eE1/Apolipoproteins complex

A 26 Å structure of Con1 eE1 357 apolipoproteins complex fits the structure of a human ApoA-I dimer ring and nE1 structure. ApoA-I dimer structure is shown in blue and the nE1 structure is in red. ApoA-I forms the ring-like structure, while eE1 takes up the space in the middle of the ring.

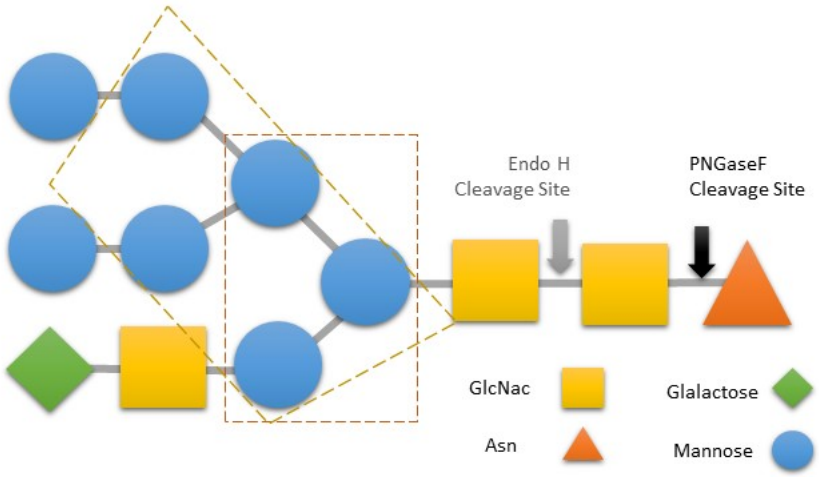

Figure 15: The Cleavage Sites of Endo H and PNGaseF

The arrows show the locations of the cleavage sites on the hybrid high mannose glycan structure. The N-linked common core is shown in red box and the glycans produced by GnTI^{-} cells is shown in brown box.

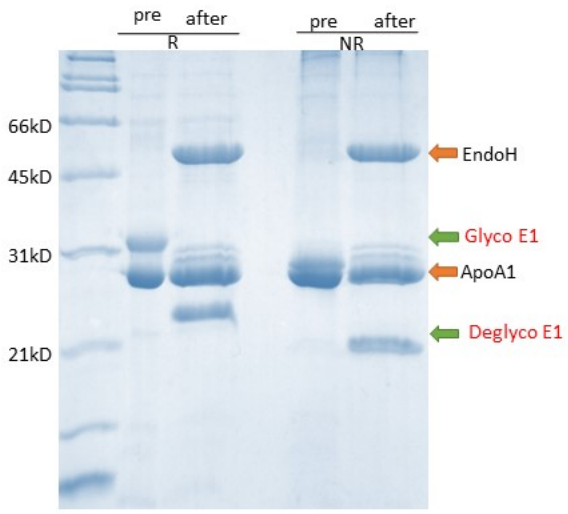

Figure 16: SDS-PAGE of eE1 before and after the Deglycosylation

The sample were with both reducing (R) and non-reducing (NR) conditions after four hours of Endo H treatment.

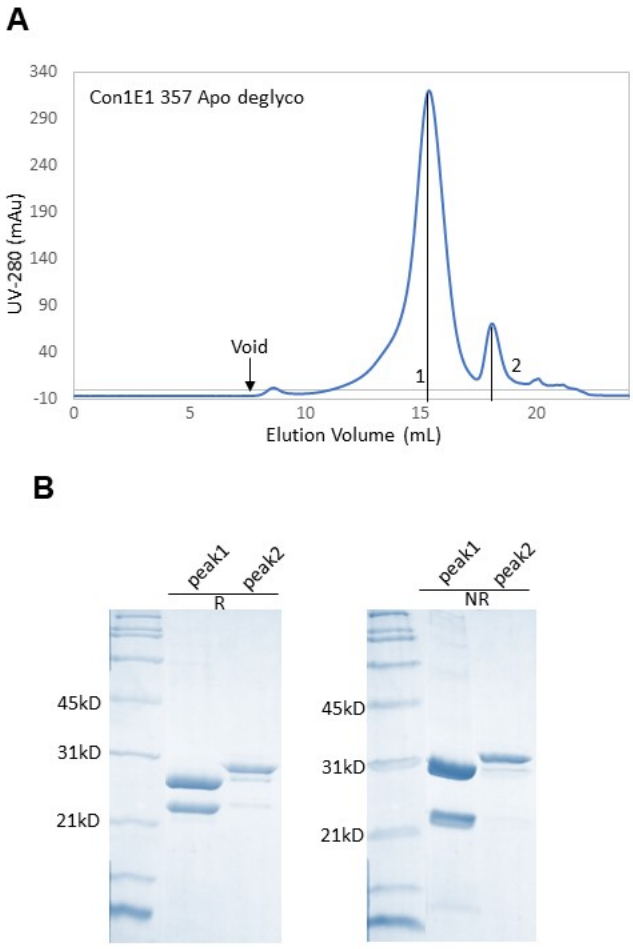

Figure 17: Post-deglycosylation Purification on eE1/Apolipoproteins

(A) SEC profile of deglycosylated eE1/Apolipoproteins complex. The elution buffer for SEC is 20 mM HEPES pH 7.5 with 100 mM NaCl.
(B) SDS-PAGE of the post-SEC first and second peak under reducing (R) and non-reducing (NR) conditions.

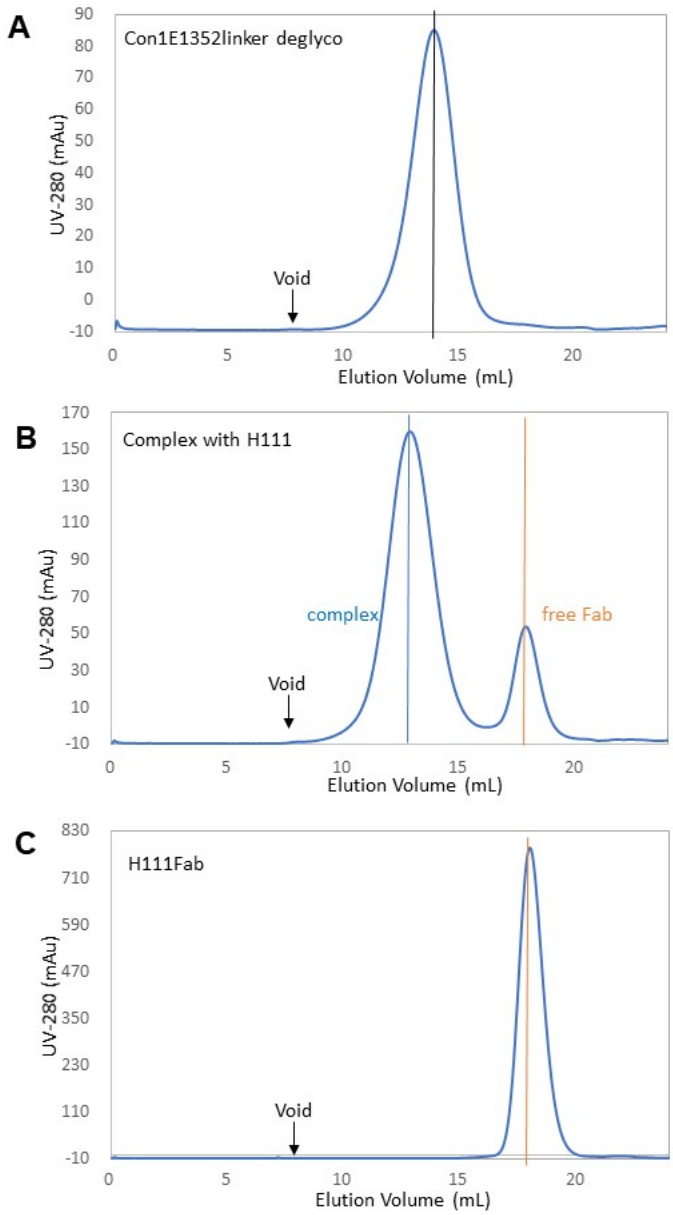

Figure 18: The SEC of eE1, Fab, and the Complex

(A) The SEC of Con1 eE1 352 linker deglycosylated protein. (B) The SEC of the complex of deglycosylated Con1 eE1 352 linker with the Fab fragment of human neutralizing antibody H111. (C) The SEC of H111 Fab alone. The void volume is shown by the arrow. The elution buffer contains 20 mM HEPES pH 7.5 and 100 mM NaCl. The elution volume of main peak in (B) shows a difference as the elution volume (A), suggesting a larger particle size for the samples in (B). The elution buffer for SEC is 20 mM HEPES pH 7.5 with 100 mM NaCl.

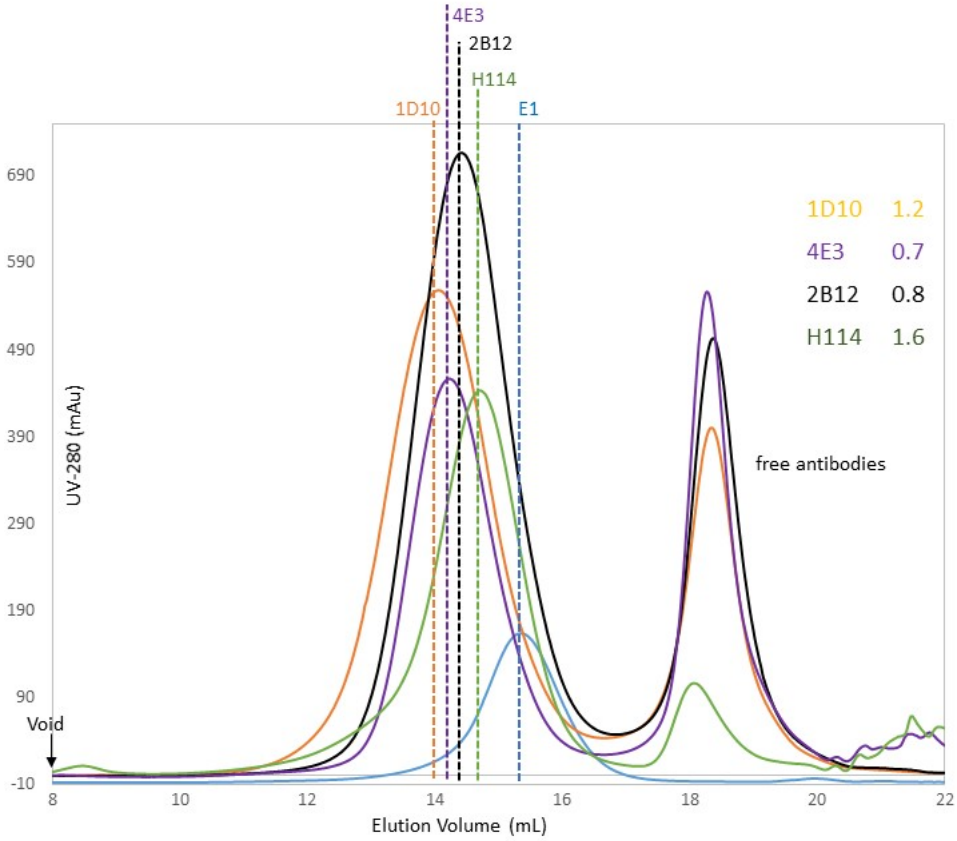

Figure 19: Overlay of the SEC Profiles of Different Antibodies Binding

The full-glycosylated Con1 eE1 357 was complexed with the Fab fragment of mouse antibody 1D10, 4E3, 2B12, and human antibody H114 respectively. The elution buffer contains 20 mM HEPES pH 7.5 and 100 mM NaCl. The molar ratio of E1 to antibodies binding is shown. The elution buffer for SEC is 20 mM HEPES pH 7.5 with 100 mM NaCl.

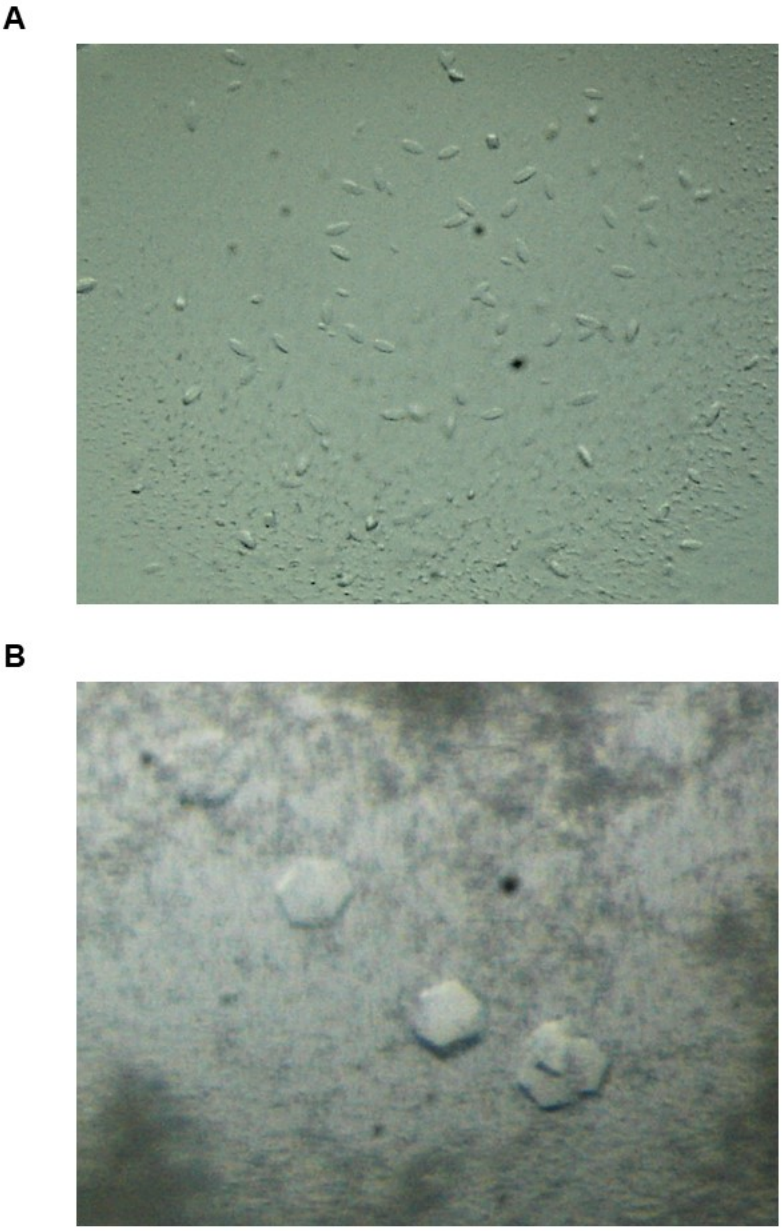

Figure 20: The Crystals of eE1/Apolipoproteins with Fab

(A) Deglycosylated Con eE1 352 linker with H-111 Fab fragment was complexed and concentrated to 10 mg/mL. The crystal was grown at 20 °C from a 96-well sitting drop screening. The crystallization solution consists of 4% v/v Tacsimate pH 4.0 and 12% w/v Polyethylene glycol 3,350. The very small football-shaped crystal starts form after 20 days. The size of the crystals is around 20 μm.

(B) Fully glycosylated Con eE1 357 with 2B12 Fab fragment was complexed and concentrated to 9 mg/mL. The crystal was grown at 20 °C from a 24-well hanging drop screening. The crystallization solution consists of 0.1 M ammonium sulfate and 20% w/v Polyethylene glycol 4,000. The 400 μm-sized hexagonal prisms-shaped crystals were form overnight and grew bigger in the following three days.

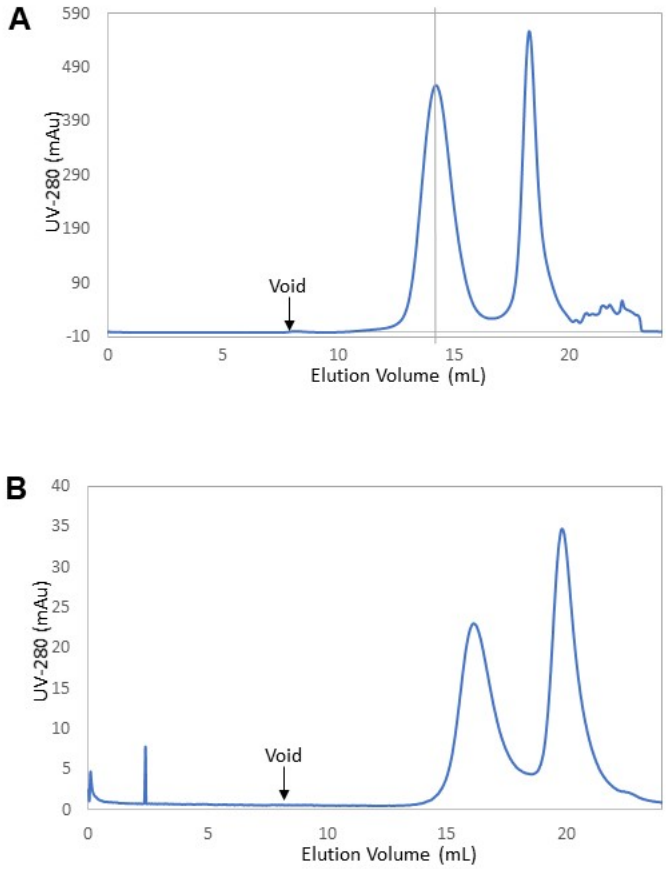

Figure 21: Complex Dissociation Test by SEC

(A) The SEC profile on fully glycosylated Con1 E1 357 with 2B12-G10 Fab. The fist peak is the complex and the second the the excess antibody. The elution buffer for SEC is 20 mM HEPES pH 7.5 with 100 mM NaCl.
(B)The complexed protein purified on (A) is applied on SEC with the 20 mM sodium acetate pH 5.0 and 100 mM NaCl, showing two peaks of the complex dissociation.

Figure 22: The Crystal Structure of human CD81-LEL

CD81-LEL is at a homodimeric form with a mushroom-like conformation. (PDB ID: 1G8Q)

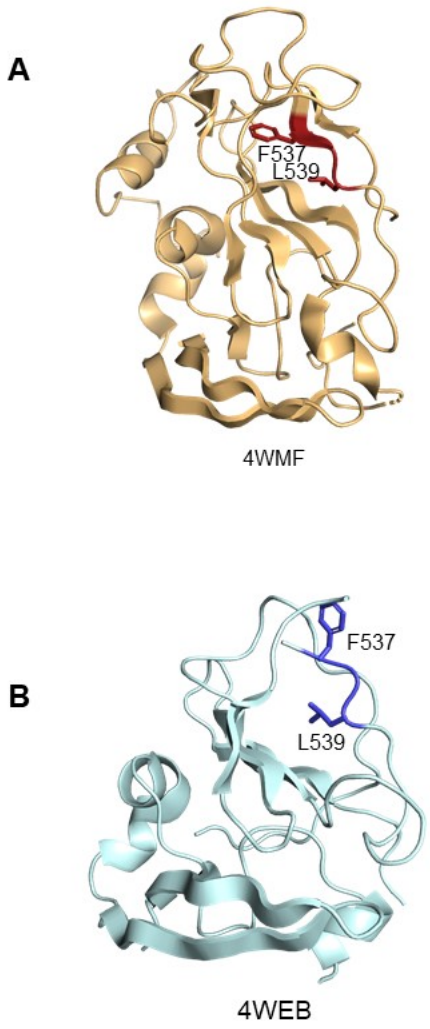

Figure 23: E2 Hydrophobic Residue Positions in CD81 Binding Loop

(A)E2 residue F537 and L539 (side chains are shown as red sticks) are stabilized by Fab fragment with flipping into the hydrophobic core. (PDB ID: 4MWF)
(B)Solvent exposed positions of residue F537 and L539 (side chains are shown as blue sticks). (PDB ID: 4WEB)

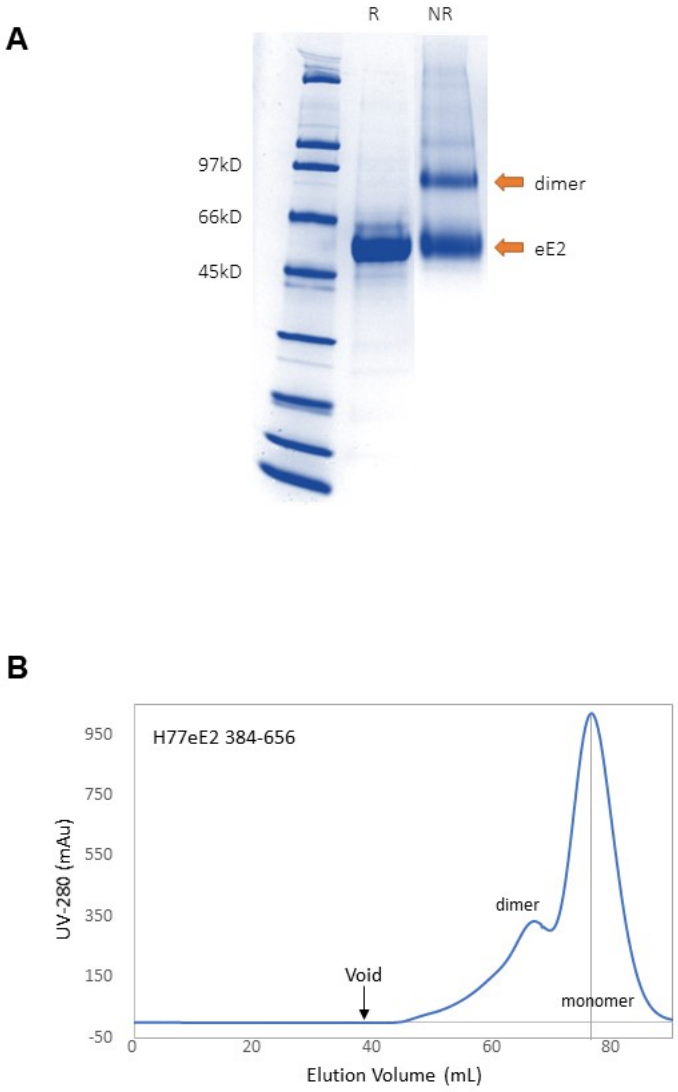

Figure 24: Oligomeric Analysis of eE2 by SDS-PAGE and SEC

(A) SDS-PAGE of fully glycosylated J6 full-length eEL with reducing (R) and non-reducing (NR) conditions. The disulfide-linked high oligomers can be shown on the Coomassie-stained non-reducing gel with higher molecular weight bands. The monomer eE2 is around 45 kDa and dimer is around 90 kDa.
(B) SEC profile of fully-glycosylated H77 full-length eE2 with 20 mM HEPES pH 7.5 and 100 mM NaCl as the elution buffer.

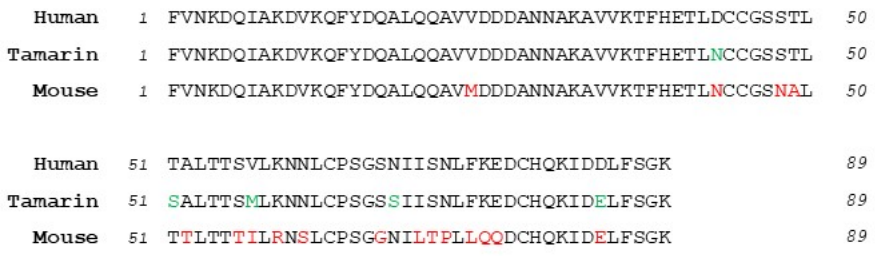

Figure 25: Sequence Alignment on Human, Tamarin, and Mouse CD81-LEL

Sequence Alignment on Human, Tamarin, and Mouse CD81-LEL. The difference in sequence are in green (between human and tamarin) and red (between human and mouse).

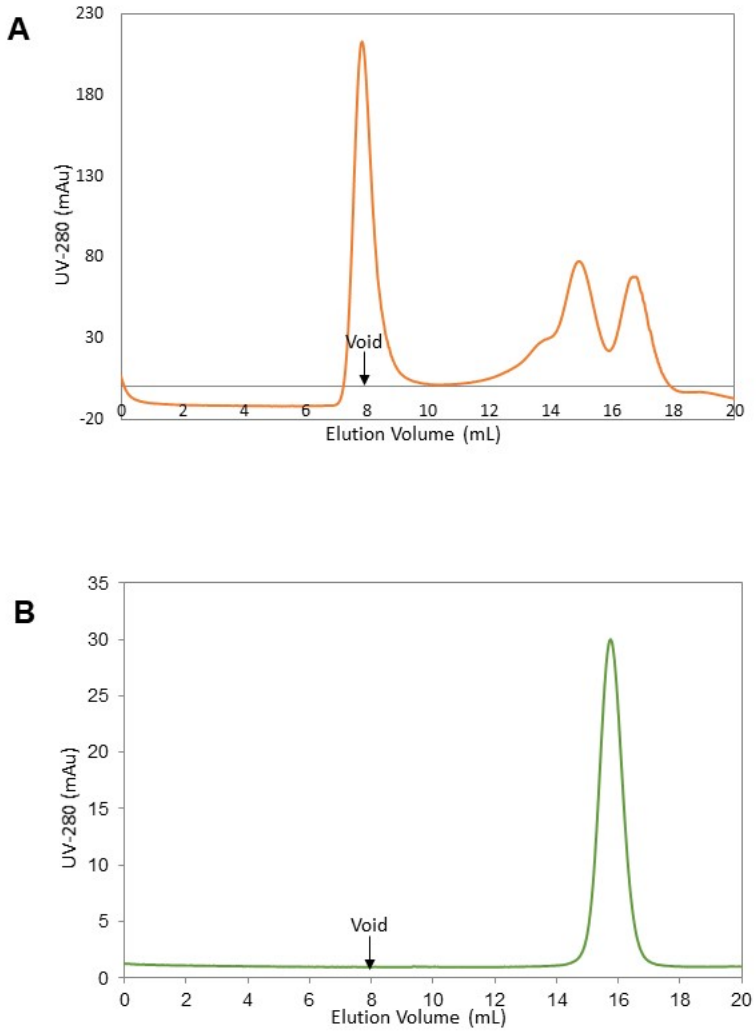

Figure 26: SEC Profile of CD81-LEL Expressed in Different Systems

The human CD81-LEL is expressed in both bacteria (A) and mammalian cells (B). Most of the protein from bacteria culture aggregates, while the rest is under different oligomeric forms. The SEC of the CD81-LEL in mammalian culture has a single, symmetric peak with a dimeric form. The elution buffer of SEC is 20 mM HEPES pH 7.5 with 100 mM NaCl.

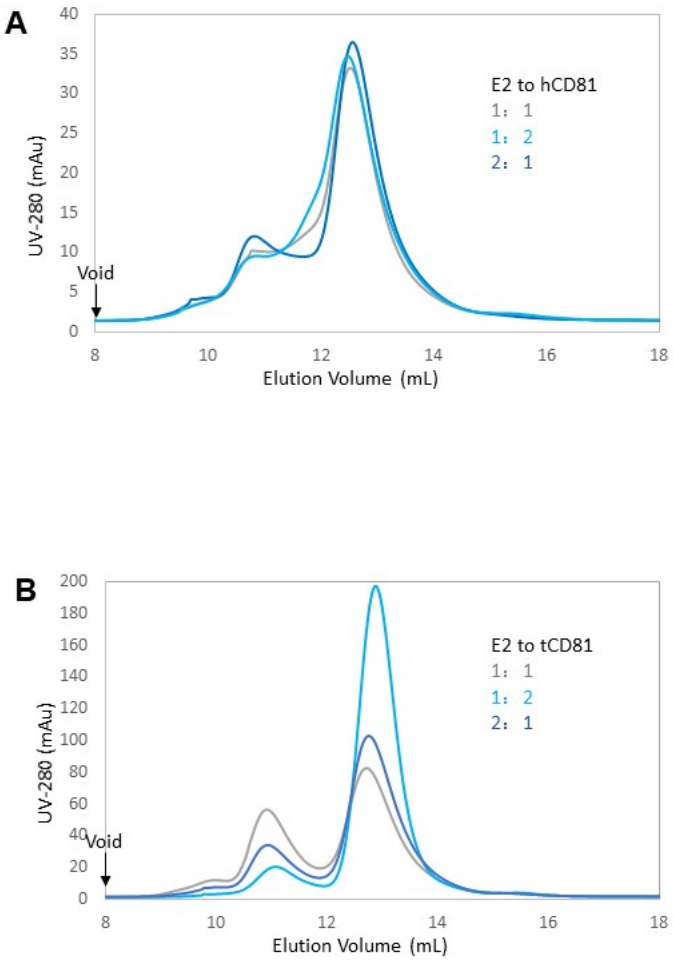

Figure 27: SEC Profiles of eE2 and CD81-LEL Complexes

Different molar ratios (1:1, 2:1, 1:2) of the purified fully-glycosylated J6 full-length eE2 mixed with human (A) or tamarin (B) CD81-LEL followed by SEC. The elution buffer of SEC is 20 mM HEPES pH 7.5 with 100 mM NaCl. The E2/CD81 complex is at the elution volume of 11 mL, while E2 is at 13 mL.

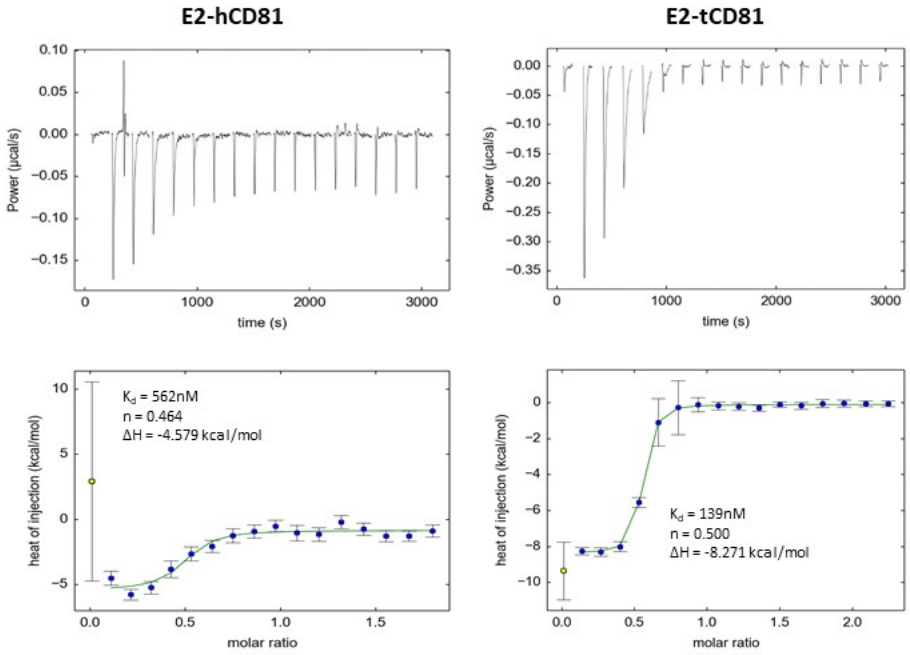

Figure 28: ITC Analysis of E2 and CD81 Interaction

Fully glycosylated J6 eE2FL was in the cell at around 15 µM, and CD81 was in the syringe at around 100 µM. The sample from syringe was injected to the cell for 17 times by 0.2 µL for the first one followed by 2.35 µL each, while stirring at 750 rpm for mixing. The binding constant (K_d), stoichiometry (n), and enthalpy of binding (ΔH) are shown.

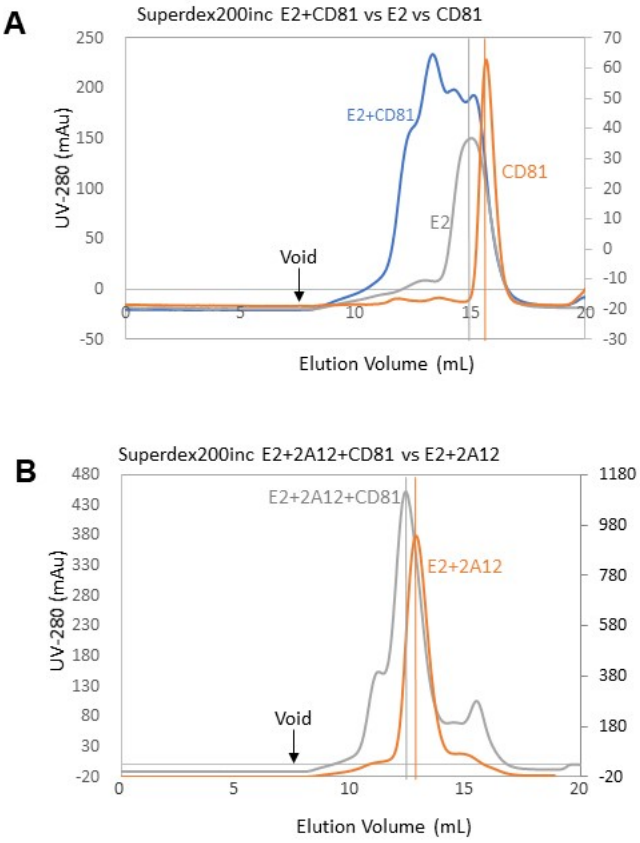

Figure 29: SEC Analysis of E2-CD81 Interaction with the Presence of Antibody

(A)SEC profile of fully-glycosylated H77 eE2FL was shown in grey, while human CD81-LEL was in orange, and the complex formed at 1:1 molar ratio is in blue.
(B)E2 was complex with 2A12 first followed by mixing with CD81. E2-2A12-CD81 complex is shown in grey and E2-1A12 complex is shown in orange. The elution buffer contains 20 mM HEPES pH 7.5 and 100 mM NaCl.

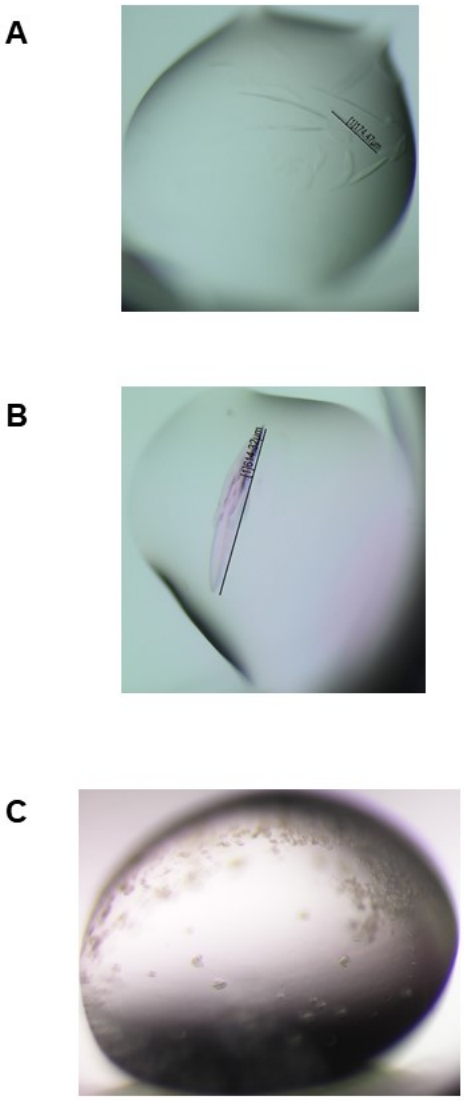

Figure 30: Crystals of eE2FL with tCD81

Crystallization conditions are (A)0.1M Sodium acetate trihydrate pH4.5, 20% w/v PEG 10,000, (B)0.1M MES monohydrate pH6.0, 14% PEG 4000, and (C)0.2 M Zinc acetate dihydrate, 20% w/v Polyethylene glycol 3,350

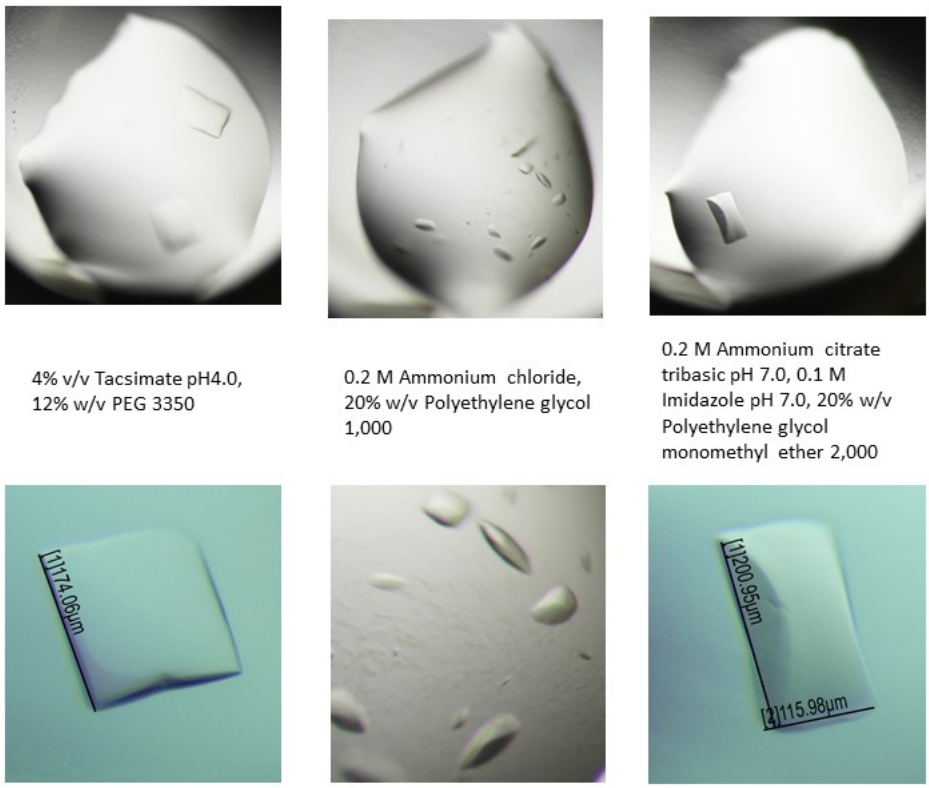

Figure 31: Crystals of eE2 ΔHVR1 with tCD81

The crystallization conditions are shown between the overview and zoom-in images.

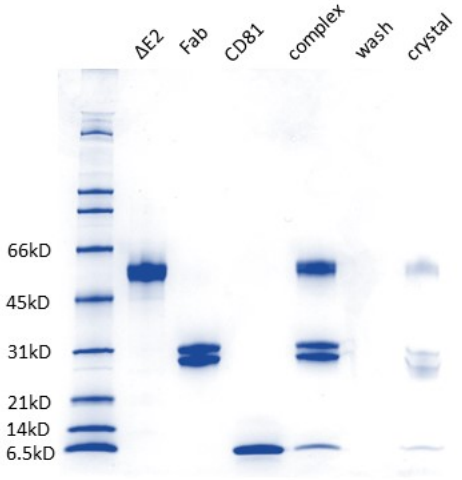

Figure 32: The SDS-PAGE of the Crystals

Around 10 crystals were transferred to a new drop of mother liquor solution to remove the traces of the protein solution. The transfer step was then repeated for 3-4 times to wash the crystal surfaces. The washed crystals were dissolved in SDS-PAGE sample reducing buffer, followed by loading onto an SDS-PAGE.

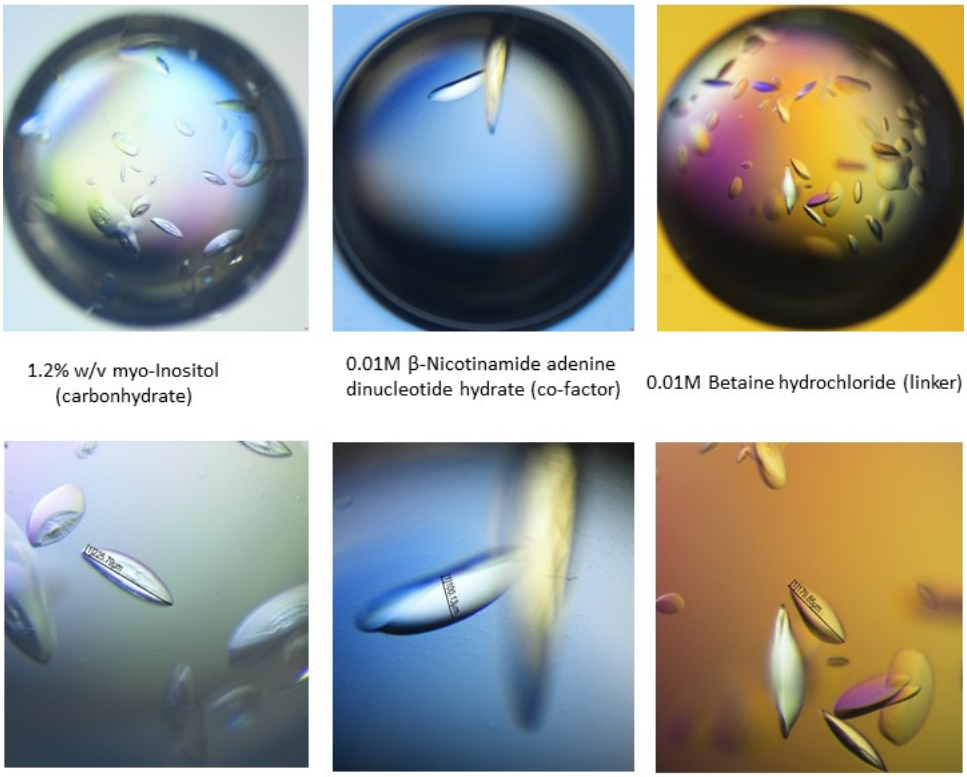

Figure 33: Additive Screening of the Crystals

Additive screening (Hampton Research) was set up with 24-well VDX plate using the same crystallization reagent. One µL of the sample was added onto the cover slide followed by 0.8 µL of the crystallization reagent and 0.2 µL of the additive. For the volatile reagent, the additive was added directly to the well solution followed by sealing the reservoir. The crystallization conditions are shown I between the overview and zoom-in images with the original condition of 0.2 M Sodium acetate trihydrate pH 4.6 and 14% PEG 3,350.

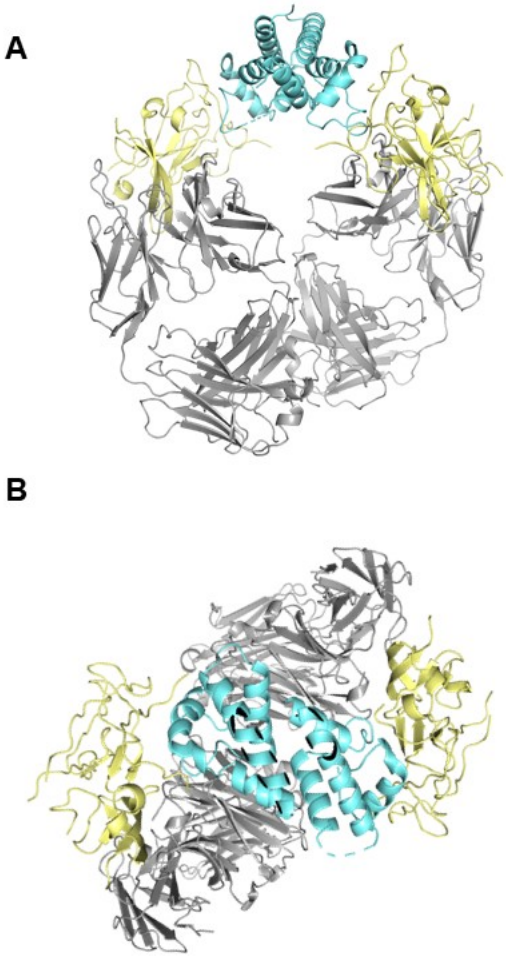

Figure 34: The Crystal Structure of E2 in Complex with Antibody and CD81

The structure is shown in front (A) and top (B) view. E2 is shown in yellow, CD81 is in blue, and Fab is shown in grey.

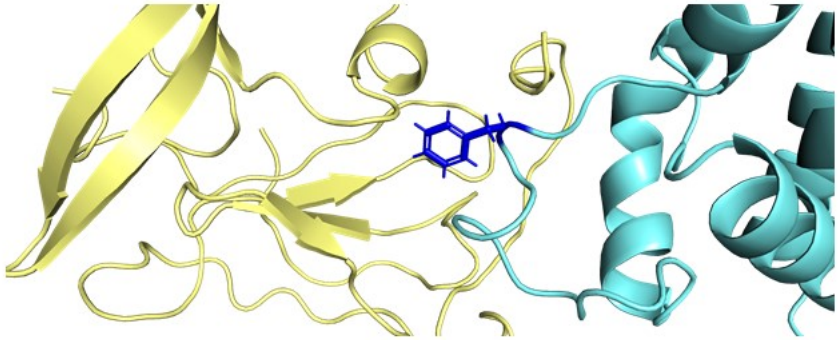

Figure 35: The Conformational Change of CD81 Binding Loop

Phe186 residue on CD81 (in blue) with the side chain, is at the E2/CD81 binding interface.

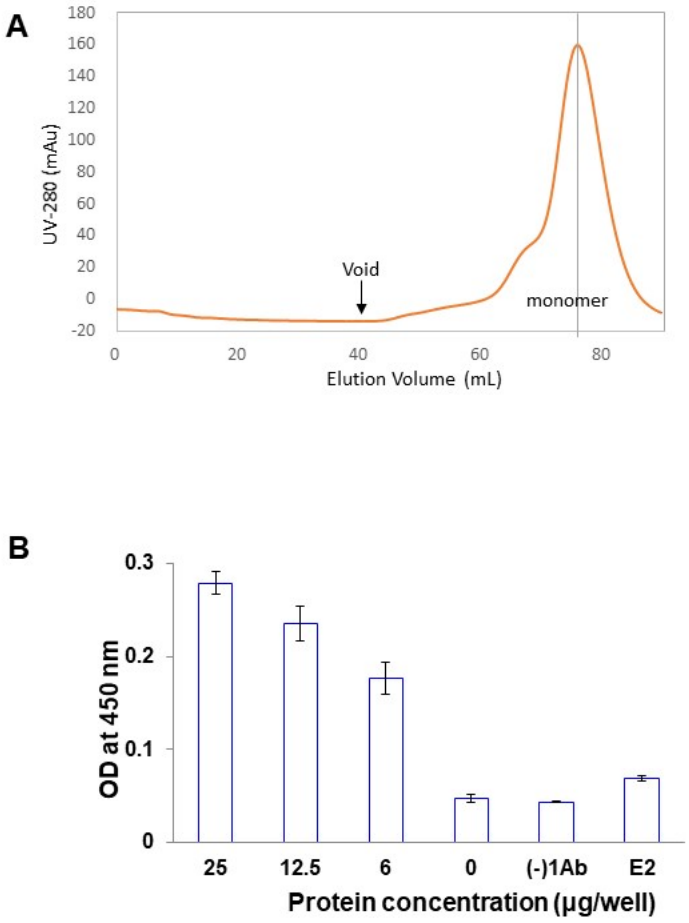

Figure 36: SEC and ELISA analysis on SRB1

(A) SEC of fully-glycosylated human eSRB1 with 20 mM HEPES pH 7.5 and 250 mM NaCl as the elution buffer, showing a monomeric form in solution.
(B)ELISA result of human eSRB1 with different concentration and the human monoclonal antibodies. E2 is a negative control.

Table 1: The Production Level of Different E1 Constructs

Construct	Production (mg/L media)
Con1 eE1 352 linker	9
Con1 eE1 311 linker	4
Con1 eE1 330 linker	5
Con1 eE1 342 linker	6
Con1 eE1 352	8
Con1 eE1 357	9
J6 eE1 356	1

Table 2: The Common Components Found in Different Genotypes of eE1 by Mass Spectrometry

Protein	Residue numbers of mature proteoforms	Longest from the N-terminus	Longest from the C-terminus
P15497 Apolipoprotein A-I (Bovine)	19-265 25-265 25-264	25-152	153-265
P81644 Apolipoprotein A-II (Bovine)	19-100 24-100 24-99	24-99	24-99
P34955 Alpha-1-antiproteinase (Bovine)	25-416	179-225	339-416
P02081 Hemoglobin fetal subunit beta (Bovine)	1-145	1-50	93-145
P02070 Hemoglobin subunit beta (Bovine)	1-145	1-30	
P12763 Alpha-2-HS-glycoprotein	19-359	252-266	348-348
Q2KIH2 ApoN protein (Bovine)	19-254	167-179	218-254
P01966 Hemoglobin subunit alpha (Bovine)	2-142	88-123	92-128
P01888 Beta-2-macroglobulin (Bovine)	21-118	21-118	21-118
Q9TTE1 Serpin A3-1 (Bovine)	25-411		375-411

Table 3: The Overall Procedure of Mouse Monoclonal Antibody Generation

Stage	Description	Time line
Immunization	Monoclonal antibody production, phase I, 10 animal immunization with conventional protocol	8-10 weeks
Cell fusion	Monoclonal antibody production, phase I, 10 animal immunization with conventional protocolMonoclonal antibody production, phase II, cell fusion, supernatants of 50-70 clones delivery	6-8 weeks
Subcloning	Monoclonal antibody production, phase III, subcloning, expansion and cryopreservation, 6-10 cell lines subcloning	6-8 weeks

Table 4: Anti-E1 Antibody Purification and Digestion

Antibodies	Origin	Binding	Production of FL	Sub-cloned
1D2	Mouse	330; 357	14.6 mg/L; 3 mg/L Fab	
1D10	Mouse	nE1; 330 357	13 mg/L; 2.05 mg/L Fab	
1G7	Mouse	330	none	
2B9			none	2B9-A5: none
2C1	Mouse	330	10 mg/L	2C1-1A: 5.2 mg/L
2E4	Mouse	330	7 mg/L	
2F2	Mouse	nE1; 330 Weak on 303; no 357 biding	17.5 mg/L; 3.3 mg/L Fab	
2F7	Mouse	Weak on nE1 and 303; cE1, 311 H77; no 357 biding	23 mg/L; 4.5 mg/L Fab	
2F11				2F11-D1: none
2G9				2G9-G2: none
2B12		357	24 mg/L; 2.7 mg/L Fab	2B12-D1: none
2B12-G10: 9.2 g/L				
3C1	Mouse	Weak on nE1; 330	9.8 mg/L; 0.75 mg/L Fab	
3D2	Mouse	H77	3.6 mg/L	
3E8	Mouse	Weak on nE1 and 303; 330	4.2 mg/L	
3F5			21 mg/L	
3G7			1.8 mg/L	
4D4	Mouse	330		
4E3	Mouse	330; 357	18 mg/L; 2.7 mg/L Fab	
H111	Human	nE1; 357	9.28 mg/L; 2.25 mg/L Fab	
H114	Human	nE1; 311 357	53 mg/L; 23 mg/L Fab	

Table 5: Anti-E1 Antibody Purification and Digestion

Antibody	Clone	FL Yield (mg)	Digestion Time (h)	Fab Yield/L (mg)	Remarks about Fab
H111	6B3	7.2	5	1.469	In ProA FT, In MonoQ FT
H114		159.7	5	23.4	In ProA FT, In MonoQ FT
2F7	G12	69	3	4.48	In ProA FT, Clean In MonoQ FT
4E3		53.1	3	2.73	In ProA FT, Binds weakly to MonoQ
2F2		20.5	2	3.3375	In ProA FT, In MonoQ FT
3C1		1.4	2	0.04625	Use ProG NOT ProA
1D10		50.2	4	2.0475	Used ProG NOT ProA, Binds MonoQ
2B12	G10	48	3	2.725	Used ProG NOT ProA, Binds MonoQ, GF before freezing
1D2		20.8	3	3	ProAProG Tandem, Mono Q 0-10% B in 30 min

Table 6: The Crystallization Trial on eE1 and Different Antibodies

Complex Commercial Kit Screening at 4 °C and 20 °C	H111	H114	1D2	1D10	2B12	4E3
352 linker deglyco	Index Crystal PEG/Ion	Index Crystal PEG/Ion PEG Rx Gras 1-4	Index Crystal PEG/Ion	Index Crystal PEG/Ion	Index Crystal PEG/Ion	
352 glyco	Index Crystal PEG/Ion	Index Crystal PEG/Ion				Index Crystal PEG/Ion
352 deglyco		Index Crystal PEG/Ion Gras 1-4				Index Crystal PEG/Ion Gras 1-4
357 glyco		Index Crystal PEG/Ion Gras 1-4 Salt		Index Crystal PEG/Ion Gras 1-4	Index Crystal PEG/Ion Gras 1-4 Salt	Index Crystal PEG/Ion Gras 1-4 Salt
357 deglyco	Index Crystal PEG/Ion	Index Crystal PEG/Ion Gras 1-4 Salt				

Table 7: The Crystal Conditions of Full-length eE2/Fab/CD81-LEL

Condition	Crystal First Seen After	Temp
0.1M Sodium acetate trihydrate pH4.5, 20% w/v PEG 10,000	2 days	4
0.1M MES monohydrate pH6.0, 14% PEG 4000	2 days	4
0.2 M Zinc acetate dihydrate, 20% w/v Polyethylene glycol 3,350	3 days	20

Table 8: The Crystal Conditions of ΔHVR1 eE2/Fab and/CD81-LEL

Condition	Crystal First Seen After	Temp
4% v/v Tacsimate pH4.0, 12% w/v PEG 3350	1 day	4
0.1M Sodium acetate trihydrate pH4.6, 2% v/v Tacsimate pH 4.0,16% PEG 3350	1 day	4
0.1M MES monohydrate pH6.0, 14% PEG 4000	1 day	4
0.1 M Sodium acetate trihydrate pH 4.6, 2% v/v Tacsimate pH 4.0, 16% w/v Polyethylene glycol 3,350	4 days	20
0.1 M Sodium acetate trihydrate pH 4.5, 10% w/v Polyethylene glycol 10,000	4 days	4
2% v/v 1,4-Dioxane, 0.1 M Tris pH 8.0, 15% w/v Polyethylene glycol 3,350	4 days	4
0.1 M Ammonium tartrate dibasic pH 7.0, 12% w/v Polyethylene glycol 3,350	4 days	4
(0.07 M Citric acid, 0.03 M BIS-TRIS propane)/pH 3.4, 16% w/v Polyethylene glycol 3,350	4 days	4
0.2 M Ammonium chloride, 20% w/v Polyethylene glycol 1,000	4 days	4
4% v/v Tacsimate pH 8.0, 12% w/v Polyethylene glycol 3,350	11 days	4
0.2 M Ammonium citrate tribasic pH 7.0, 0.1 M Imidazole pH 7.0, 20% w/v Polyethylene glycol monomethyl ether 2,000	11 days	4

Conclusion

HCV infection is a growing public health problem, as an increasing number of young people are infected due to a growing number of injection drug users. The vaccine is not available for HCV yet and the current therapy is very costly. HCV glycoproteins play an important role during the HCV entry, which could be a potential target for vaccine design.

The previous study on the function and conformation of HCV E1 was hindered by the difficulty of getting the properly folded protein. Thus, the function and role of E1 during membrane fusion process remains unidentified. As far as I know, we are the first group who can produce milligrams of properly folded functional full-length ectodomain of HCV E1. We have successfully developed a method to produce recombinant glycoproteins in mammalian cell lines with native, posttranslational modifications. The technology combines a lentiviral expression system to produce a high-expressing, stable cell line with a three-dimensional adherent cell bioreactor. Glycoproteins will be produced in an HEK293T cell line that lacks N-acetylglucos-aminyltransferase I (GnTI) activity, resulting in homogenous glycans. HCV is characterized to be shield by different apolipoproteins and lipoproteins. From the mass spectrometry result of E1, several apolipoproteins could interact with E1 to form a large complex particle which could be visualized by negative-stain electron microscope. Moreover, cholesterol and cholesterol ester is crucial for virus infection which has been founded in the E1 complex we produced. The further study is needed on measuring the amount of cholesterol interacted with E1. More monoclonal antibodies were generated against eE1 192-357 proteins, which could be a useful tool for further functional and structural studies. The crystallographic studies of E1 in complexed with apolipoproteins are ongoing with some preliminary crystals. The recombinant E1 protein we produced has opened a window to establish more collaborative studies.

Scavenger Receptor Class B Type I (SRB1) and Cluster of Differentiation 81 (CD81) are both identified to undergo the physical interaction with HCV E2, although the underlying mechanism of binding is unclear. For the SRB1 and E2 interaction, it is still lack of evidence of the binding affinity or conformational change during the entry. The binding affinity of E2 and CD81 is determined by ITC, but the stoichiometry remains unclear. The crystal of E2 in complex with CD81 and antibody was determined at a 4.3 Å resolution. From the structure, the CD81 dimer can interact with two monomeric E2. The optimization of the complex crystals is undergoing seeking for a better diffraction pattern to obtain the atomic resolution.

HCV glycoproteins have a function as fusion protein during the HCV entry, which may undergo the conformational and oligomeric state rearrangement at low-pH. Neither of E1 nor E2 alone was detected to undergo a conformational change, which brings the question on whether E1E2 together could function as the fusion protein. The recombinant protein of E1E2 with the transmembrane region was successfully expressed and in the process of optimizing the purification method.

Overall, a better understanding of HCV lifecycle and the mechanism of HCV entry would concrete a solid foundation for antiviral interception and therapeutic development. The crystal structure of CD81 with E2 is critical for vaccine design and obtaining an atomic resolution structure of the complex.

Bibliography

[1] QL Choo, G Kuo, AJ Weiner, LR Overby, DW Bradley, and M Houghton. Isolation of a cDNA clone derived from a blood-borne non-A, non-B viral hepatitis genome. *Science*, 244(4902):359–362, 1989.

[2] G Kuo, QL Choo, HJ Alter, GL Gitnick, AG Redeker, RH Purcell, T Miyamura, JL Dienstag, MJ Alter, CE Stevens, and al. et. An assay for circulating antibodies to a major etiologic virus of human non-A, non-B hepatitis. *Science*, 244(4902):362–364, 1989.

[3] Division of Viral Hepatitis, STD National Center for HIV/AIDS, Viral Hepatitis, and TB Prevention. Hepatitis C Questions and Answers for the Public, 2018.

[4] World Health Organization. Hepatitis C, 2017.

[5] Brian R Edlin, Benjamin J Eckhardt, Marla A Shu, Scott D Holmberg, and Tracy Swan. Toward a more accurate estimate of the prevalence of hepatitis C in the United States. *Hepatology*, 62(5):1353–1363, 2015.

[6] Marc G. Ghany, David R. Nelson, Doris B. Strader, David L. Thomas, and Leonard B. Seeff. An update on treatment of genotype 1 chronic hepatitis C virus infection: 2011 practice guideline by the American Association for the Study of Liver Diseases. *Hepatology*, 54(4):1433–1444.

[7] Jon E Zibbell, Kashif Iqbal, Rajiv C Patel, Anil Suryaprasad, Kathy J Sanders, Loretta Moore-Moravian, Jamie Serrecchia, Steven Blankenship, John W Ward, and Deborah Holtzman. Increases in hepatitis C virus infection related to injection drug use among persons aged 30 years-Kentucky, Tennessee, Virginia, and West Virginia, 2006-2012. *MMWR. Morbidity and mortality weekly report*, 64(17):453–458, 2015.

[8] Margaret Hellard, Rachel Sacks-Davis, and Judy Gold. Hepatitis C Treatment for Injection Drug Users: A Review of the Available Evidence. *Clinical Infectious Diseases*, 49(4):561–573, 2009.

[9] Donald B Smith, Jens Bukh, Carla Kuiken, A Scott Muerhoff, Charles M Rice, Jack T Stapleton, and Peter Simmonds. Expanded classification of hepatitis C virus into 7 genotypes and 67 subtypes: updated criteria and genotype assignment web resource. *Hepatology*, 59(1):318–327, 2014.

[10] Mohamed S Abdel-Hakeem and Naglaa H Shoukry. Protective immunity against hepatitis C: many shades of gray. *Frontiers in immunology*, 5:274, 2014.

[11] Guan Qiang and Ravi Jhaveri. Lipid droplet binding of hepatitis C virus core protein genotype 3. *ISRN gastroenterology*, 2012, 2012.

[12] Thomas von Hahn and Charles M Rice. Hepatitis C virus entry. *Journal of Biological Chemistry*, 283(7):3689–3693, 2008.

[13] Davor Pavlović, David CA Neville, Olivier Argaud, Baruch Blumberg, Raymond A Dwek, Wolfgang B Fischer, and Nicole Zitzmann. The hepatitis C virus p7 protein forms an ion channel that is inhibited by long-alkyl-chain iminosugar derivatives. *Proceedings of the National Academy of Sciences*, 100(10):6104–6108, 2003.

[14] Ivo C Lorenz, Joseph Marcotrigiano, Thomas G Dentzer, and Charles M Rice. Structure of the catalytic domain of the hepatitis C virus NS2-3 protease. *Nature*, 442(7104):831, 2006.

[15] Denise Egger, Benno Wölk, Rainer Gosert, Leonardo Bianchi, Hubert E Blum, Darius Moradpour, and Kurt Bienz. Expression of hepatitis C virus proteins induces distinct membrane alterations including a candidate viral replication complex. *Journal of virology*, 76(12):5974–5984, 2002.

[16] Jun Kato, Naoya Kato, Hideo Yoshida, Suzane Kioko Ono-Nita, Yasushi Shiratori, and Masao Omata. Hepatitis C virus NS4A and NS4B proteins suppress translation in vivo. *Journal of medical virology*, 66(2):187–199, 2002.

[17] Nobuyuki Enomoto, I Sakuma, Y Asahina, M Kurosaki, T Murakami, C Yamamoto, N Izumi, F Marumo, and C Sato. Comparison of full-length sequences of interferon-sensitive and resistant hepatitis C virus 1b. Sensitivity to interferon is conferred by amino acid substitutions in the NS5A region. *The Journal of clinical investigation*, 96(1):224–230, 1995.

[18] Maria Teresa Catanese, Kunihiro Uryu, Martina Kopp, Thomas J Edwards, Linda

Andrus, William J Rice, Mariena Silvestry, Richard J Kuhn, and Charles M Rice. Ultrastructural analysis of hepatitis C virus particles. *Proceedings of the National Academy of Sciences*, 110(23):9505–9510, 2013.

[19] Andreas Merz, Gang Long, Marie-Sophie Hiet, Britta Brügger, Petr Chlanda, Patrice Andre, Felix Wieland, Jacomine Krijnse-Locker, and Ralf Bartenschlager. Biochemical and morphological properties of hepatitis C virus particles and determination of their lipidome. *Journal of Biological Chemistry*, 286(4):3018–3032, 2011.

[20] P Andre, F Komurian-Pradel, S Deforges, M Perret, JL Berland, M Sodoyer, S Pol, C Brechot, G Paranhos-Baccala, and V Lotteau. Characterization of low- and very-low-density hepatitis C virus RNA-containing particles. *Journal of virology*, 76(14):6919–6928, 2002.

[21] Laurence Cocquerel, Czeslaw Wychowski, Frederic Minner, François Penin, and Jean Dubuisson. Charged residues in the transmembrane domains of hepatitis C virus glycoproteins play a major role in the processing, subcellular localization, and assembly of these envelope proteins. *Journal of virology*, 74(8):3623–3633, 2000.

[22] Amélie Choukhi, Sophana Ung, Czeslaw Wychowski, and Jean Dubuisson. Involvement of endoplasmic reticulum chaperones in the folding of hepatitis C virus glycoproteins. *Journal of virology*, 72(5):3851–3858, 1998.

[23] Abdul Ghafoor Khan, Jillian Whidby, Matthew T Miller, Hannah Scarborough, Alexandra V Zatorski, Alicja Cygan, Aryn A Price, Samantha A Yost, Caitlin D Bohannon, Joshy Jacob, et al. Structure of the core ectodomain of the hepatitis C virus envelope glycoprotein 2. *Nature*, 509(7500):381, 2014.

[24] Jean Dubuisson and Charles M Rice. Hepatitis C virus glycoprotein folding: disulfide bond formation and association with calnexin. *Journal of virology*, 70(2):778–786, 1996.

[25] Leopold Kong, Erick Giang, Travis Nieusma, Rameshwar U. Kadam, Kristin E. Cogburn, Yuanzi Hua, Xiaoping Dai, Robyn L. Stanfield, Dennis R. Burton, Andrew B. Ward, Ian A. Wilson, and Mansun Law. Hepatitis C Virus E2 Envelope Glycoprotein Core Structure. *Science*, 342(6162):1090–1094, 2013.

[26] Kamel El Omari, Oleg Iourin, Jan Kadlec, Geoff Sutton, Karl Harlos, Jonathan M

Grimes, and David I Stuart. Unexpected structure for the N-terminal domain of hepatitis C virus envelope glycoprotein E1. *Nature communications*, 5:4874, 2014.

[27] Brian G Pierce, Zhen-Yong Keck, Patrick Lau, Catherine Fauvelle, Ragul Gowthaman, Thomas F Baumert, Thomas R Fuerst, Roy A Mariuzza, and Steven KH Foung. Global mapping of antibody recognition of the hepatitis C virus E2 glycoprotein: Implications for vaccine design. *Proceedings of the National Academy of Sciences*, 113(45):E6946–E6954, 2016.

[28] Liang-Tzung Lin, Ting-Ying Chen, Song-Chow Lin, Chueh-Yao Chung, Ta-Chen Lin, Guey-Horng Wang, Robert Anderson, Chun-Ching Lin, and Christopher D Richardson. Broad-spectrum antiviral activity of chebulagic acid and punicalagin against viruses that use glycosaminoglycans for entry. *BMC microbiology*, 13(1):187, 2013.

[29] M Mahmood Hussain, Dudley K Strickland, and Ahmed Bakillah. The mammalian low-density lipoprotein receptor family. *Annual review of nutrition*, 19(1):141–172, 1999.

[30] Elisa Scarselli, Helenia Ansuini, Raffaele Cerino, Rosa Maria Roccasecca, Stefano Acali, Gessica Filocamo, Cinzia Traboni, Alfredo Nicosia, Riccardo Cortese, and Alessandra Vitelli. The human scavenger receptor class B type I is a novel candidate receptor for the hepatitis C virus. *The EMBO journal*, 21(19):5017–5025, 2002.

[31] Viet Loan Dao Thi, Christelle Granier, Mirjam B Zeisel, Maryse Guérin, Jimmy Mancip, Ophélia Granio, François Penin, Dimitri Lavillette, Ralf Bartenschlager, Thomas F Baumert, et al. Characterization of hepatitis C virus particle subpopulations reveals multiple usage of the scavenger receptor BI for entry steps. *Journal of Biological Chemistry*, pages jbc–M112, 2012.

[32] Michela Brazzoli, Alessia Bianchi, Sara Filippini, Amy Weiner, Qing Zhu, Mariagrazia Pizza, and Stefania Crotta. CD81 is a central regulator of cellular events required for hepatitis C virus infection of human hepatocytes. *Journal of virology*, 82(17):8316–8329, 2008.

[33] Matthew J Evans, Thomas von Hahn, Donna M Tscherne, Andrew J Syder, Maryline Panis, Benno Wölk, Theodora Hatziioannou, Jane A McKeating, Paul D Bieniasz, and Charles M Rice. Claudin-1 is a hepatitis C virus co-receptor required for a late

step in entry. *Nature*, 446(7137):801, 2007.

[34] Marion Sourisseau, Maria L Michta, Chati Zony, Benjamin Israelow, Sharon E Hopcraft, Christopher M Narbus, Ana Parra Martín, and Matthew J Evans. Temporal analysis of hepatitis C virus cell entry with occludin directed blocking antibodies. *PLoS pathogens*, 9(3):e1003244, 2013.

[35] Florian Douam, Dimitri Lavillette, and François-Loïc Cosset. The mechanism of HCV entry into host cells. In *Progress in molecular biology and translational science*, volume 129, pages 63–107. Elsevier, 2015.

[36] Margaret Kielian. Class II virus membrane fusion proteins. *Virology*, 344(1):38–47, 2006.

[37] Nishi R Sharma, Guaniri Mateo, Marlene Dreux, Arash Grakoui, Francois Loic Cosset, and Gregory B Melikyan. Hepatitis C virus is primed by CD81 for low pH-dependent fusion. *Journal of Biological Chemistry*, pages jbc–M111, 2011.

[38] Borries Demeler. UltraScan: a comprehensive data analysis software package for analytical ultracentrifugation experiments. *Modern analytical ultracentrifugation: techniques and methods*, pages 210–229, 2005.

[39] Raymond C Stevens. High-throughput protein crystallization. *Current opinion in structural biology*, 10(5):558–563, 2000.

[40] Jens Rudolph, Matthias Lormann, Carsten Bolm, and Stefan Dahmen. A high-throughput screening approach for the determination of additive effects in organozinc addition reactions to aldehydes. *Advanced Synthesis & Catalysis*, 347(10):1361–1368, 2005.

[41] Baila Samreen, Saba Khaliq, Usman Ali Ashfaq, Mahwish Khan, Nadeem Afzal, Muhammad Aiman Shahzad, Sabeen Riaz, and Shah Jahan. Hepatitis C virus entry: role of host and viral factors. *Infection, Genetics and Evolution*, 12(8):1699–1709, 2012.

[42] Dimitri Lavillette, Eve-Isabelle Pécheur, Peggy Donot, Judith Fresquet, Jennifer Molle, Romuald Corbau, Marlène Dreux, François Penin, and François-Loïc Cosset. Characterization of fusion determinants points to the involvement of three discrete regions of both E1 and E2 glycoproteins in the membrane fusion process of hepatitis

C virus. *Journal of virology*, 81(16):8752–8765, 2007.

[43] Laurence Cocquerel, Chiung-Chi Kuo, Jean Dubuisson, and Shoshana Levy. CD81-dependent binding of hepatitis C virus E1E2 heterodimers. *Journal of virology*, 77(19):10677–10683, 2003.

[44] Laurence Cocquerel, Elizabeth R Quinn, Mike Flint, Kenneth G Hadlock, Steven KH Foung, and Shoshana Levy. Recognition of native hepatitis C virus E1E2 heterodimers by a human monoclonal antibody. *Journal of virology*, 77(2):1604–1609, 2003.

[45] Marlène Dreux, Thomas Pietschmann, Christelle Granier, Cécile Voisset, Sylvie Ricard-Blum, Philippe-Emmanuel Mangeot, Zhenyong Keck, Steven Foung, Ngoc Vu-Dac, Jean Dubuisson, et al. High density lipoprotein inhibits hepatitis C virus neutralising antibodies by stimulating cell entry via activation of the scavenger receptor BI. *Journal of Biological Chemistry*, 2006.

[46] Zhen-Yong Keck, Ta-Kai Li, Jinming Xia, Birke Bartosch, François-Loïc Cosset, Jean Dubuisson, and Steven KH Foung. Analysis of a highly flexible conformational immunogenic domain a in hepatitis C virus E2. *Journal of virology*, 79(21):13199–13208, 2005.

[47] Leopold Kong, Rameshwar U Kadam, Erick Giang, Tinashe B Ruwona, Travis Nieusma, Jeffrey C Culhane, Robyn L Stanfield, Philip E Dawson, Ian A Wilson, and Mansun Law. Structure of hepatitis C virus envelope glycoprotein E1 antigenic site 314–324 in complex with antibody IGH526. *Journal of molecular biology*, 427(16):2617–2628, 2015.

[48] Jean Dubuisson, Henry H Hsu, Ramsey C Cheung, Harry B Greenberg, David G Russell, and Charles M Rice. Formation and intracellular localization of hepatitis C virus envelope glycoprotein complexes expressed by recombinant vaccinia and Sindbis viruses. *Journal of virology*, 68(10):6147–6160, 1994.

[49] Mansun Law, Toshiaki Maruyama, Jamie Lewis, Erick Giang, Alexander W Tarr, Zania Stamataki, Pablo Gastaminza, Francis V Chisari, Ian M Jones, Robert I Fox, et al. Broadly neutralizing antibodies protect against hepatitis C virus quasispecies challenge. *Nature medicine*, 14(1):25, 2008.

[50] Jean Dubuisson, Sandrine Duvet, Jean-Christophe Meunier, Anne Op De Beeck, Rene

Cacan, Czeslaw Wychowski, and Laurence Cocquerel. Glycosylation of the hepatitis C virus envelope protein E1 is dependent on the presence of a downstream sequence on the viral polyprotein. *Journal of Biological Chemistry*, 275(39):30605–30609, 2000.

[51] Janisha Patel, Arvind H Patel, and John McLauchlan. The transmembrane domain of the hepatitis C virus E2 glycoprotein is required for correct folding of the E1 glycoprotein and native complex formation. *Virology*, 279(1):58–68, 2001.

[52] Tae Kyung Kim and James H Eberwine. Mammalian cell transfection: the present and the future. *Analytical and bioanalytical chemistry*, 397(8):3173–3178, 2010.

[53] Luigi Naldini, Ulrike Blömer, Philippe Gallay, Daniel Ory, Richard Mulligan, Fred H Gage, Inder M Verma, and Didier Trono. In vivo gene delivery and stable transduction of nondividing cells by a lentiviral vector. *Science*, 272(5259):263–267, 1996.

[54] Pierre Falson, Birke Bartosch, Khaled Alsaleh, Birke Andrea Tews, Antoine Loquet, Yann Ciczora, Laura Riva, Cédric Montigny, Claire Montpellier, Gilles Duverlie, et al. Hepatitis C virus envelope glycoprotein E1 forms trimers at the surface of the virion. *Journal of virology*, pages JVI–00991, 2015.

[55] Laurence Cocquerel, Sandrine Duvet, Jean-Christophe Meunier, André Pillez, René Cacan, Czeslaw Wychowski, and Jean Dubuisson. The transmembrane domain of hepatitis C virus glycoprotein E1 is a signal for static retention in the endoplasmic reticulum. *Journal of virology*, 73(4):2641–2649, 1999.

[56] Matteo Castelli, Nicola Clementi, Jennifer Pfaff, Giuseppe A Sautto, Roberta A Diotti, Roberto Burioni, Benjamin J Doranz, Matteo Dal Peraro, Massimo Clementi, and Nicasio Mancini. A biologically-validated HCV E1E2 heterodimer structural model. *Scientific reports*, 7(1):214, 2017.

[57] Peter Hüssy, Georg Schmid, Jan Mous, and Helmut Jacobsen. Purification and in vitro-phospholabeling of secretory envelope proteins E1 and E2 of hepatitis C virus expressed in insect cells. *Virus research*, 45(1):45–57, 1996.

[58] JP Michalak, C Wychowski, A Choukhi, JC Meunier, S Ung, CM Rice, and J Dubuisson. Characterization of truncated forms of hepatitis C virus glycoproteins. *Journal of General Virology*, 78(9):2299–2306, 1997.

[59] Roberta Spadaccini, Gerardino D'Errico, Viviana D'Alessio, Eugenio Notomista,

Alessia Bianchi, Marcello Merola, and Delia Picone. Structural characterization of the transmembrane proximal region of the hepatitis C virus E1 glycoprotein. *Biochimica et Biophysica Acta (BBA)-Biomembranes*, 1798(3):344–353, 2010.

[60] Yoshiharu Matsuura, Tetsuro Suzuki, Ryosuke Suzuki, Mitsuru Sato, Hideki Aizaki, Izumu Saito, and Tatsuo Miyamura. Processing of E1 and E2 glycoproteins of hepatitis C virus expressed in mammalian and insect cells. *Virology*, 205(1):141–150, 1994.

[61] Irene Boo, Florian Douam, Dimitri Lavillette, Pantelis Poumbourios, Heidi E Drummer, et al. Distinct roles in folding, CD81 receptor binding and viral entry for conserved histidine residues of hepatitis C virus glycoprotein E1 and E2. *Biochemical Journal*, 443(1):85–94, 2012.

[62] Emilie Crouchet, Thomas F Baumert, and Catherine Schuster. Hepatitis C virus–apolipoprotein interactions: molecular mechanisms and clinical impact. *Expert review of proteomics*, 14(7):593–606, 2017.

[63] Vassilis I Zannis, Panagiotis Fotakis, Georgios Koukos, Dimitris Kardassis, Christian Ehnholm, Matti Jauhiainen, and Angeliki Chroni. HDL biogenesis, remodeling, and catabolism. In *High Density Lipoproteins*, pages 53–111. Springer, 2015.

[64] Hiro-Omi Mowri, Josef R Patsch, Antonio M Gotto Jr, and Wolfgang Patsch. Apolipoprotein A-II influences the substrate properties of human HDL2 and HDL3 for hepatic lipase. *Arteriosclerosis, thrombosis, and vascular biology*, 16(6):755–762, 1996.

[65] Indra Ramasamy. Recent advances in physiological lipoprotein metabolism. *Clinical Chemistry and Laboratory Medicine (CCLM)*, 52(12):1695–1727, 2014.

[66] Stéphane Bressanelli, Karin Stiasny, Steven L Allison, Enrico A Stura, Stéphane Duquerroy, Julien Lescar, Franz X Heinz, and Félix A Rey. Structure of a flavivirus envelope glycoprotein in its low-ph-induced membrane fusion conformation. *The EMBO journal*, 23(4):728–738, 2004.

[67] Anne Op De Beeck, Cécile Voisset, Birke Bartosch, Yann Ciczora, Laurence Cocquerel, Zhenyong Keck, Steven Foung, François-Loïc Cosset, and Jean Dubuisson. Characterization of functional hepatitis C virus envelope glycoproteins. *Journal of virology*, 78(6):2994–3002, 2004.

[68] S Shire. Determination of molecular weight of glycoproteins by analytical ultracentrifugation. *Technical Note DS-837. Palo Alto, CA: Beckman*, 1992.

[69] John Stirling, Alan Curry, and Brian Eyden. *Diagnostic electron microscopy: A practical guide to interpretation and technique*. John Wiley & Sons, 2013.

[70] David W Borhani, Danise P Rogers, Jeffrey A Engler, and Christie G Brouillette. Crystal structure of truncated human apolipoprotein AI suggests a lipid-bound conformation. *Proceedings of the National Academy of Sciences*, 94(23):12291–12296, 1997.

[71] Ken F. Jarrell, Yan Ding, Benjamin H. Meyer, Sonja-Verena Albers, Lina Kaminski, and Jerry Eichler. N-Linked Glycosylation in Archaea: a Structural, Functional, and Genetic Analysis. *Microbiology and Molecular Biology Reviews*, 78(2):304–341, 2014.

[72] JC Meunier, A Fournillier, A Choukhi, A Cahour, L Cocquerel, J Dubuisson, and C Wychowski. Analysis of the glycosylation sites of hepatitis C virus (HCV) glycoprotein E1 and the influence of E1 glycans on the formation of the HCV glycoprotein complex. *Journal of General Virology*, 80(4):887–896, 1999.

[73] A Fournillier, C Wychowski, D Boucreux, TF Baumert, J-C Meunier, D Jacobs, S Muguet, E Depla, and G Inchauspe. Induction of hepatitis C virus E1 envelope protein-specific immune response can be enhanced by mutation of N-glycosylation sites. *Journal of virology*, 75(24):12088–12097, 2001.

[74] Elodie Beaumont, Emmanuelle Roch, Lucie Chopin, and Philippe Roingeard. Hepatitis C Virus E1 and E2 proteins used as separate immunogens induce neutralizing antibodies with additive properties. *PloS one*, 11(3):e0151626, 2016.

[75] Jean-Christophe Meunier, Rodney S Russell, Vera Goossens, Sofie Priem, Hugo Walter, Erik Depla, Ann Union, Kristina N Faulk, Jens Bukh, Suzanne U Emerson, et al. Isolation and characterization of broadly neutralizing human monoclonal antibodies to the e1 glycoprotein of hepatitis C virus. *Journal of virology*, 82(2):966–973, 2008.

[76] Zhen-Yong Keck, Vicky MH Sung, Susan Perkins, Judy Rowe, Sudhir Paul, T Jake Liang, Michael MC Lai, and Steven KH Foung. Human monoclonal antibody to hepatitis C virus E1 glycoprotein that blocks virus attachment and viral infectivity. *Journal of virology*, 78(13):7257–7263, 2004.

[77] Jan M Pestka, Mirjam B Zeisel, Edith Bläser, Peter Schürmann, Birke Bartosch, Francois-Loïc Cosset, Arvind H Patel, Helga Meisel, Jens Baumert, Sergei Viazov, et al. Rapid induction of virus-neutralizing antibodies and viral clearance in a single-source outbreak of hepatitis C. *Proceedings of the National Academy of Sciences*, 104(14):6025–6030, 2007.

[78] Shohei Koide. Engineering of recombinant crystallization chaperones. *Current opinion in structural biology*, 19(4):449–457, 2009.

[79] L Griffin and A Lawson. Antibody fragments as tools in crystallography. *Clinical & Experimental Immunology*, 165(3):285–291, 2011.

[80] Andrew J Prongay, Thomas J Smith, Michael G Rossmann, Lorna S Ehrlich, Carol A Carter, and Jan McClure. Preparation and crystallization of a human immunodeficiency virus p24-Fab complex. *Proceedings of the National Academy of Sciences*, 87(24):9980–9984, 1990.

[81] Brett D Lindenbach, Matthew J Evans, Andrew J Syder, Benno Wölk, Timothy L Tellinghuisen, Christopher C Liu, Toshiaki Maruyama, Richard O Hynes, Dennis R Burton, Jane A McKeating, et al. Complete replication of hepatitis C virus in cell culture. *Science*, 309(5734):623–626, 2005.

[82] Zhen-yong Keck, Jinming Xia, Yong Wang, Wenyan Wang, Thomas Krey, Jannick Prentoe, Thomas Carlsen, Angela Ying-Jian Li, Arvind H Patel, Stanley M Lemon, et al. Human monoclonal antibodies to a novel cluster of conformational epitopes on HCV E2 with resistance to neutralization escape in a genotype 2a isolate. *PLoS pathogens*, 8(4):e1002653, 2012.

[83] RACHEL Oren, Shuji Takahashi, Carol Doss, Rx Levy, and S Levy. TAPA-1, the target of an antiproliferative antibody, defines a new family of transmembrane proteins. *Molecular and cellular biology*, 10(8):4007–4015, 1990.

[84] Shoshana Levy, Scott C Todd, and Holden T Maecker. CD81 (TAPA-1): a molecule involved in signal transduction and cell adhesion in the immune system. *Annual review of immunology*, 16(1):89–109, 1998.

[85] Kengo Kitadokoro, Domenico Bordo, Giuliano Galli, Roberto Petracca, Fabiana

Falugi, Sergio Abrignani, Guido Grandi, and Martino Bolognesi. CD81 extracellular domain 3D structure: insight into the tetraspanin superfamily structural motifs. *The EMBO Journal*, 20(1-2):12–18, 2001.

[86] Adrian Higginbottom, Elizabeth R Quinn, Chiung-Chi Kuo, Mike Flint, Louise H Wilson, Elisabetta Bianchi, Alfredo Nicosia, Peter N Monk, Jane A McKeating, and Shoshana Levy. Identification of amino acid residues in CD81 critical for interaction with hepatitis C virus envelope glycoprotein E2. *Journal of virology*, 74(8):3642–3649, 2000.

[87] Roberto Petracca, Fabiana Falugi, Giuliano Galli, Nathalie Norais, Domenico Rosa, Susanna Campagnoli, Vito Burgio, Enrico Di Stasio, Bruno Giardina, Michael Houghton, et al. Structure-function analysis of hepatitis C virus envelope-CD81 binding. *Journal of virology*, 74(10):4824–4830, 2000.

[88] Heidi E Drummer, Kirilee A Wilson, and Pantelis Poumbourios. Identification of the hepatitis C virus E2 glycoprotein binding site on the large extracellular loop of CD81. *Journal of Virology*, 76(21):11143–11147, 2002.

[89] Piero Pileri, Yasushi Uematsu, Susanna Campagnoli, Giuliano Galli, Fabiana Falugi, Roberto Petracca, Amy J Weiner, Michael Houghton, Domenico Rosa, Guido Grandi, et al. Binding of hepatitis C virus to CD81. *Science*, 282(5390):938–941, 1998.

[90] Lucie Fénéant, Shoshana Levy, and Laurence Cocquerel. CD81 and hepatitis C virus (HCV) infection. *Viruses*, 6(2):535–572, 2014.

[91] Ieva Vasiliauskaite, Ania Owsianka, Patrick England, Abdul Ghafoor Khan, Sarah Cole, Dorothea Bankwitz, Steven KH Foung, Thomas Pietschmann, Joseph Marcotrigiano, Felix A Rey, et al. Conformational flexibility in the immunoglobulin-like domain of the hepatitis C virus glycoprotein E2. *MBio*, 8(3):e00382–17, 2017.

[92] Mike Flint, Jean Dubuisson, Catherine Maidens, Richard Harrop, Geoffrey R Guile, Persephone Borrow, and Jane A McKeating. Functional characterization of intracellular and secreted forms of a truncated hepatitis C virus E2 glycoprotein. *Journal of virology*, 74(2):702–709, 2000.

[93] Kathleen McCaffrey, Hamed Gouklani, Irene Boo, Pantelis Poumbourios, and Heidi E Drummer. The variable regions of hepatitis C virus glycoprotein E2 have an essential

structural role in glycoprotein assembly and virion infectivity. *Journal of General Virology*, 92(1):112–121, 2011.

[94] Michelle C Sabo, Vincent Luca, Jannick Prentoe, Sharon E Hopcraft, Keril J Blight, MinKyung Yi, Stanley M Lemon, Jonathan K Ball, Jens Bukh, Matthew J Evans, et al. Neutralizing monoclonal antibodies against hepatitis c virus e2 protein bind discontinuous epitopes and inhibit infection at a post-attachment step. *Journal of virology*, pages JVI–00586, 2011.

[95] Barbara Rehermann, Kyong-Mi Chang, J McHutchinson, Robert Kokka, Michael Houghton, Charles M Rice, and Francis V Chisari. Differential cytotoxic T-lymphocyte responsiveness to the hepatitis B and C viruses in chronically infected patients. *Journal of Virology*, 70(10):7092–7102, 1996.

[96] Tobias Allander, Xavier Forns, Suzanne U Emerson, Robert H Purcell, and Jens Bukh. Hepatitis C virus envelope protein E2 binds to CD81 of tamarins. *Virology*, 277(2):358–367, 2000.

[97] Jean-Philippe Julien, Albert Cupo, Devin Sok, Robyn L. Stanfield, Dmitry Lyumkis, Marc C. Deller, Per-Johan Klasse, Dennis R. Burton, Rogier W. Sanders, John P. Moore, Andrew B. Ward, and Ian A. Wilson. Crystal structure of a soluble cleaved hiv-1 envelope trimer. *Science*, 2013.

[98] Marie Pancera, Syed Shahzad-ul Hussan, Nicole A Doria-Rose, Jason S McLellan, Robert T Bailer, Kaifan Dai, Sandra Loesgen, Mark K Louder, Ryan P Staupe, Yongping Yang, et al. Structural basis for diverse n-glycan recognition by hiv-1–neutralizing v1–v2–directed antibody pg16. *Nature structural & molecular biology*, 20(7):804, 2013.

[99] Mark R Wormald and Raymond A Dwek. Glycoproteins: glycan presentation and protein-fold stability. *Structure*, 7(7):R155–R160, 1999.

[100] Emilia Falkowska, Francis Kajumo, Edie Garcia, John Reinus, and Tatjana Dragic. Hepatitis C virus envelope glycoprotein E2 glycans modulate entry, CD81 binding, and neutralization. *Journal of virology*, 81(15):8072–8079, 2007.

[101] S Acton, A Rigotti, K T Landschulz, S Xu, H H Hobbs, and M Krieger. Identification of scavenger receptor SR-BI as a high density lipoprotein receptor. *Science (New*

York, N.Y.), 271(5248):518–20, Jan 1996.

[102] Teemu J Murtola, Heimo Syvälä, Pasi Pennanen, Merja Bläuer, Tiina Solakivi, Timo Ylikomi, and Teuvo L J Tammela. The importance of LDL and cholesterol metabolism for prostate epithelial cell growth. *PloS one*, 7(6):e39445, 2012.

[103] Shuo Yang, Marina G Damiano, Heng Zhang, Sushant Tripathy, Andrea J Luthi, Jonathan S Rink, Andrey V Ugolkov, Amareshwar T K Singh, Sandeep S Dave, Leo I Gordon, and C Shad Thaxton. Biomimetic, synthetic HDL nanostructures for lymphoma. *Proceedings of the National Academy of Sciences of the United States of America*, 110(7):2511–6, Feb 2013.

[104] Ying Zheng, Yanyan Liu, Honglin Jin, Shaotao Pan, Yuan Qian, Chuan Huang, Yixin Zeng, Qingming Luo, Musheng Zeng, and Zhihong Zhang. Scavenger receptor B1 is a potential biomarker of human nasopharyngeal carcinoma and its growth is inhibited by HDL-mimetic nanoparticles. *Theranostics*, 3(7):477, 2013.

[105] Attilio Rigotti, Helena E Miettinen, and Monty Krieger. The role of the high-density lipoprotein receptor SR-BI in the lipid metabolism of endocrine and other tissues. *Endocrine reviews*, 24(3):357–87, Jun 2003.

[106] Manali Bhave, Nausheen Akhter, and Steven T Rosen. Cardiovascular toxicity of biologic agents for cancer therapy. *Oncology (Williston Park, N.Y.)*, 28(6):482–90, Jun 2014.

[107] M Krieger. Charting the fate of the "good cholesterol": identification and characterization of the high-density lipoprotein receptor SR-BI. *Annual review of biochemistry*, 68:523–58, 1999.

[108] Anthony P Kent and Ioannis M Stylianou. Scavenger receptor class B member 1 protein: hepatic regulation and its effects on lipids, reverse cholesterol transport, and atherosclerosis. *Hepatic medicine: evidence and research*, 3:29, 2011.

[109] Dante Neculai, Michael Schwake, Mani Ravichandran, Friederike Zunke, Richard F Collins, Judith Peters, Mirela Neculai, Jonathan Plumb, Peter Loppnau, Juan Carlos Pizarro, Alma Seitova, William S Trimble, Paul Saftig, Sergio Grinstein, and Sirano Dhe-Paganon. Structure of LIMP-2 provides functional insights with implications for SR-BI and CD36. *Nature*, 504(7478):172–6, Dec 2013.

[110] Dorothea Bankwitz, Eike Steinmann, Julia Bitzegeio, Sandra Ciesek, Martina Friesland, Eva Herrmann, Mirjam B Zeisel, Thomas F Baumert, Zhen-yong Keck, Steven K H Foung, Eve-Isabelle Pécheur, and Thomas Pietschmann. Hepatitis C virus hypervariable region 1 modulates receptor interactions, conceals the CD81 binding site, and protects conserved neutralizing epitopes. *Journal of virology*, 84(11):5751–63, Jun 2010.

[111] Tae-Hwe Heo, Song-Mi Lee, Birke Bartosch, Fran-Loïc Cosset, and Chang-Yuil Kang. Hepatitis C virus E2 links soluble human CD81 and SR-B1 protein. *Virus research*, 121(1):58–64, Oct 2006.

[112] Viet Loan Dao Thi, Christelle Granier, Mirjam B Zeisel, Maryse Guérin, Jimmy Mancip, Ophélia Granio, FranPenin, Dimitri Lavillette, Ralf Bartenschlager, Thomas F Baumert, Fran-Loïc Cosset, and Marlène Dreux. Characterization of hepatitis C virus particle subpopulations reveals multiple usage of the scavenger receptor BI for entry steps. *The Journal of biological chemistry*, 287(37):31242–57, Sep 2012.